De Novo Resistance to Epidermal Growth Factor Receptor-Tyrosine Kinase Inhibitors in *EGFR* Mutation-Positive Patients with Non-small Cell Lung Cancer

Masayuki Takeda, MD, PhD, Isamu Okamoto, MD, PhD,* Yoshihiko Fujita, PhD,† Tokuzo Arao, MD, PhD,† Hiroyuki Ito, MD, PhD,‡ Masahiro Fukuoka, MD, PhD,§ Kazuto Nishio, MD, PhD,† and Kazuhiko Nakagawa, MD, PhD**

Background: Somatic mutations in the epidermal growth factor receptor (EGFR) gene are a predictor of response to treatment with EGFR tyrosine kinase inhibitors (TKIs) in patients with non-small cell lung cancer (NSCLC). However, mechanisms of de novo resistance to these drugs in patients harboring *EGFR* mutations have remained unclear. We examined whether the mutational status of *KRAS* might be associated with primary resistance to EGFR-TKIs in *EGFR* mutation-positive patients with NSCLC.

Methods: Forty patients with NSCLC with *EGFR* mutations who were treated with gefitinib or erlotinib and had archival tissue specimens available were enrolled in the study. *KRAS* mutations were analyzed by direct sequencing.

Results: Three (7.5%) of the 40 patients had progressive disease, and two (67%) of these three individuals had both *KRAS* and *EGFR* mutations.

Conclusions: Our results suggest that *KRAS* mutation is a negative predictor of response to EGFR-TKIs in *EGFR* mutation-positive patients with NSCLC.

Key Words: Drug resistance, Epidermal growth factor receptor, KRAS, Non-small cell lung cancer, EGFR-TKI.

(*J Thorac Oncol.* 2010;5: 399–400)

A total of 40 patients with non-small cell lung cancer (NSCLC) harboring epidermal growth factor receptor (*EGFR*) mutations were treated with gefitinib (n = 36) or erlotinib (n = 4) between September 2002 and January 2009, and three patients exhibited resistance to EGFR-tyrosine kinase inhibitor (TKIs). (i) Case 1 was a 63-year-old man who had never smoked and was diagnosed with lung adenocarcinoma of stage IV. Molecular screening identified a deletion mutation in exon 19 of *EGFR*, and he had received gefitinib as the second-line therapy. Although he tolerated gefitinib well, the primary lung lesion showed slow but steady growth, and he was removed from therapy because of his progressive disease (PD) at day 58 (Figure 1*A*). (ii) Case 2 was a 69-year-old man who had never smoked, had adenocarcinoma of stage IIIB, harbored a deletion in exon 19 of *EGFR*, and was treated with erlotinib as the third-line therapy. A chest computed tomography scan on day 28 revealed enlargement of the primary lung lesion, and the case was subsequently classified as PD (Figure 1*B*). (iii) Case 3 was a 52-year-old man who was a current smoker, had lung adenocarcinoma of stage IV with left adrenal metastasis, harbored a deletion in exon 19 of *EGFR*, and received erlotinib as the fourth-line therapy. Chest computed tomography on day 32 showed enlargement of the left adrenal metastasis, resulting in a classification of PD (Figure 1*C*). Thus, these clinical data demonstrated the existence of de novo resistance to EGFR-TKIs in *EGFR* mutation-positive patients. We examined the mutational status of *KRAS* in the three patients who showed PD as their best response. An amino acid substitution at codon 12 (G12D) of *KRAS* was identified in two of these three patients (Figure 1*D–F*).

DISCUSSION

Somatic mutations of the *EGFR* gene are associated with an increased response to EGFR-TKI in patients with NSCLC. Several prospective clinical trials of EGFR-TKI treatment for patients with NSCLC with *EGFR* mutations have subsequently revealed radiographic response rates of 55 to 91%. It remains of clinical concern, however, that a small proportion of patients with NSCLC with *EGFR* mutations show de novo resistance to EGFR-TKIs and that molecular markers to predict a lack of response to these drugs remain to be identified. We have now examined *KRAS* mutation status in *EGFR* mutation-positive patients with NSCLC treated with EGFR-TKIs and found a high incidence of concomitant *KRAS* mutation in individuals who did not respond to these drugs. Our results indicate that *KRAS* mutation may be clinically useful as a negative predictive marker of sensitivity to EGFR-TKIs in patients with NSCLC with *EGFR* mutations. Previous studies have also shown that *KRAS* mutations are associated with resistance to EGFR-TKIs in patients with NSCLC and that *EGFR* and *KRAS* mutations

Departments of *Medical Oncology, †Genome Biology, and ‡Pathology, Kinki University School of Medicine, Osaka-Sayama; and §Department of Medical Oncology, Kinki University School of Medicine, Sakai Hospital, Minami-ku, Sakai, Osaka, Japan.

Disclosure: The authors declare no conflict of interest.

Address for correspondence: Isamu Okamoto, Department of Medical Oncology, Kinki University School of Medicine, 377-2 Ohno-higashi, Osaka-Sayama, Osaka 589-8511, Japan. E-mail: chi-okamoto@dotd.med.kindai.ac.jp

ISSN: 1556-0864/10/0503-0399

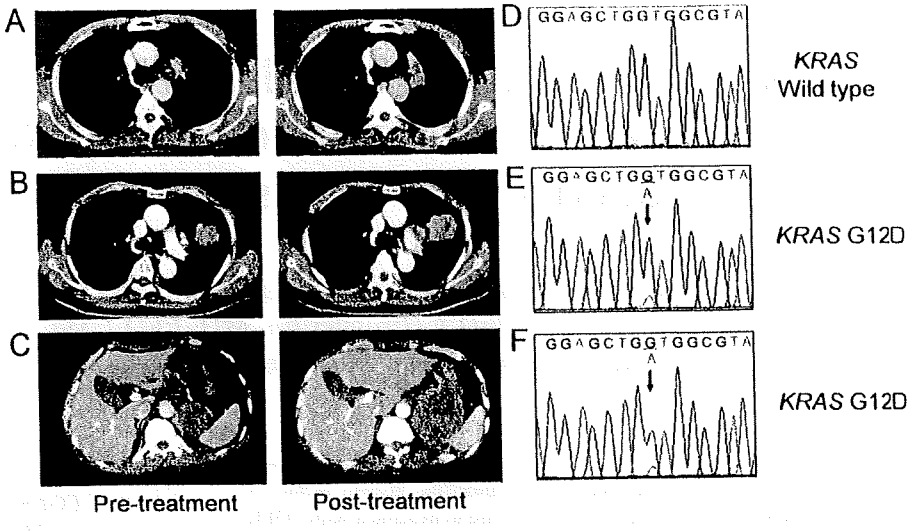

FIGURE 1. Clinical and molecular characteristics of patients with non-small cell lung cancer (NSCLC) who showed de novo resistance to epidermal growth factor receptor-tyrosine kinase inhibitors (EGFR-TKIs). *A–C*, Computed tomography (CT) images obtained before and after EGFR-TKI treatment for cases 1 to 3, respectively. *D–F*, Sequence chromatographs of *KRAS* mutation status determined with tumor tissue isolated before EGFR-TKI treatment for cases 1 to 3, respectively. Arrows indicate the mutated nucleotide (G→A) in codon 12 for cases 2 and 3.

appear to be mutually exclusive in such patients,[1–3] suggesting that *KRAS* mutations are predictors of unresponsiveness to EGFR-TKIs in patients with NSCLC with wild-type *EGFR*. The mutual exclusivity of *EGFR* and *KRAS* mutations combined with their prevalence patterns in lung adenocarcinoma, with *KRAS* mutations being preferentially found in smokers and *EGFR* mutations in nonsmokers, suggests that the mutations in these two genes might arise through different pathogenic pathways. Conversely, some studies have shown that *KRAS* mutations do sometimes coexist with *EGFR* mutations in patients with NSCLC.[4,5] The extent of coexistence of *EGFR* and *KRAS* mutations in NSCLC thus remains unclear, in large part as a result of the low frequency of *KRAS* mutations, and the clinical relevance of *KRAS* mutations in *EGFR* mutation-positive patients has remained unknown. We have now shown that patients with NSCLC harboring *EGFR* mutations who exhibit de novo resistance to EGFR-TKIs have a high incidence of *KRAS* mutation, suggesting that the presence of *KRAS* mutations might provide a basis for the identification of *EGFR* mutation-positive patients who are unlikely to benefit from EGFR-TKI treatment. Our clinical findings are consistent with preclinical data showing that forced expression of mutant KRAS in PC-9 human NSCLC cells, which harbor an activating mutation of *EGFR*, resulted in a reduction in the sensitivity of these cells to gefitinib.[6] Gefitinib shuts down both PI3K-AKT and RAS-RAF-MEK-ERK signaling pathways in PC-9 cells; however, expression of the KRAS mutant resulted in constitutive activation of these signaling pathways in a manner independent of EGFR activation, leading to continued cell growth and survival.

In July 2009, gefitinib received a license from the European Medicines Agency for all lines of therapy in patients with locally advanced or metastatic NSCLC positive for activating mutations of *EGFR*. More patients with *EGFR* mutation-positive tumors will thus now receive EGFR-TKIs. Our present results suggest that EGFR-TKIs should not be given routinely to patients harboring concomitant *KRAS* and *EGFR* mutations. In the event that such patients do receive treatment with EGFR-TKIs, they should be followed up after a short interval to obtain early evidence of possible tumor progression.

KRAS mutations cannot account for all cases of de novo resistance to EGFR-TKIs in *EGFR* mutation-positive patients with NSCLC. A recent study showed that loss of *PTEN* contributes to erlotinib resistance in an *EGFR* mutation-positive NSCLC cell line.[7] Loss of *PTEN* resulted in partial uncoupling of the mutant EGFR from downstream signaling and further activated the receptor, leading to erlotinib resistance. Both homozygous deletion of *PTEN* and *EGFR* mutation were detected in one of 24 clinical specimens of NSCLC with *EGFR* mutations, although the efficacy of EGFR-TKIs was not evaluated in the corresponding patient.

In conclusion, our results suggest that *KRAS* mutation status should be assessed before initiation of EGFR-TKI treatment in *EGFR* mutation-positive patients with NSCLC, allowing enrichment of the population of such patients who are likely to prove responsive to the treatment.

ACKNOWLEDGMENTS

The authors thank Tadao Uesugi for technical assistance.

REFERENCES

1. Shigematsu H, Lin L, Takahashi T, et al. Clinical and biological features associated with epidermal growth factor receptor gene mutations in lung cancers. *J Natl Cancer Inst* 2005;97:339–346.
2. Pao W, Wang TY, Riely GJ, et al. KRAS mutations and primary resistance of lung adenocarcinomas to gefitinib or erlotinib. *PLoS Med* 2005;2:e17.
3. Kosaka T, Yatabe Y, Endoh H, et al. Mutations of the epidermal growth factor receptor gene in lung cancer: biological and clinical implications. *Cancer Res* 2004;64:8919–8923.
4. Kalikaki A, Koutsopoulos A, Trypaki M, et al. Comparison of EGFR and K-RAS gene status between primary tumours and corresponding metastases in NSCLC. *Br J Cancer* 2008;99:923–929.
5. Han SW, Kim TY, Jeon YK, et al. Optimization of patient selection for gefitinib in non-small cell lung cancer by combined analysis of epidermal growth factor receptor mutation, K-ras mutation, and Akt phosphorylation. *Clin Cancer Res* 2006;12:2538–2544.
6. Uchida A, Hirano S, Kitao H, et al. Activation of downstream epidermal growth factor receptor (EGFR) signaling provides gefitinib-resistance in cells carrying EGFR mutation. *Cancer Sci* 2007;98:357–363.
7. Sos ML, Koker M, Weir BA, et al. PTEN loss contributes to erlotinib resistance in EGFR-mutant lung cancer by activation of Akt and EGFR. *Cancer Res* 2009;69:3256–3261.

Cancer Science
The official journal of the Japanese Cancer Association JCA

Effects of Src inhibitors on cell growth and epidermal growth factor receptor and MET signaling in gefitinib-resistant non-small cell lung cancer cells with acquired *MET* amplification

Takeshi Yoshida,[1] Isamu Okamoto,[1,6] Wataru Okamoto,[1] Erina Hatashita,[1] Yuki Yamada,[1] Kiyoko Kuwata,[1] Kazuto Nishio,[2] Masahiro Fukuoka,[3] Pasi A. Jänne[4,5] and Kazuhiko Nakagawa[1]

[1]Department of Medical Oncology, Kinki University School of Medicine, Osaka-Sayama, Osaka; [2]Department of Genome Biology, Kinki University School of Medicine, Osaka-Sayama, Osaka; [3]Department of Medical Oncology, Kinki University School of Medicine, Sakai Hospital, Minami-ku Sakai, Osaka, Japan; [4]Lowe Center for Thoracic Oncology, Dana-Farber Cancer Institute, Boston; [5]Department of Medical Oncology, Dana-Farber Cancer Institute, Boston, MA, USA

(Received August 9, 2009/Revised September 6, 2009/Accepted September 7, 2009)

The efficacy of epidermal growth factor receptor (EGFR)–tyrosine kinase inhibitors such as gefitinib and erlotinib in non-small cell lung cancer (NSCLC) is often limited by the emergence of drug resistance conferred either by a secondary T790M mutation of *EGFR* or by acquired amplification of the *MET* gene. We now show that the extent of activation of the tyrosine kinase Src is markedly increased in gefitinib-resistant NSCLC (HCC827 GR) cells with *MET* amplification compared with that in the gefitinib-sensitive parental (HCC827) cells. In contrast, the extent of Src activation did not differ between gefitinib-resistant NSCLC (PC9/ZD) cells harboring the T790M mutation of *EGFR* and the corresponding gefitinib-sensitive parental (PC9) cells. This activation of Src in HCC827 GR cells was largely abolished by the MET-TKI PHA-665752 but was only partially inhibited by gefitinib, suggesting that Src activation is more dependent on MET signaling than on EGFR signaling in gefitinib-resistant NSCLC cells with *MET* amplification. Src inhibitors blocked Akt and Erk signaling pathways, resulting in both suppression of cell growth and induction of apoptosis, in HCC827 GR cells as effectively as did the combination of gefitinib and PHA-665752. Furthermore, Src inhibitor dasatinib inhibited tumor growth in HCC827 GR xenografts to a significantly greater extent than did treatment with gefitinib alone. These results provide a rationale for clinical targeting of Src in gefitinib-resistant NSCLC with *MET* amplification. (*Cancer Sci* 2009)

Upregulation of the EGFR occurs frequently and is negatively correlated with prognosis in many types of human malignancy.[1,2] Recognition of the role of EGFR in carcinogenesis has prompted the development of EGFR-targeted therapies.[3] TKI of EGFR, such as gefitinib and erlotinib, both of which compete with ATP for binding to the tyrosine kinase pocket of the receptor, have been extensively studied in patients with NSCLC.[4] Sensitivity to these drugs has been correlated with the presence of somatic mutations that affect the kinase domain of EGFR, such as deletions in exon 19 and the L858R mutation in exon 21 of the *EGFR* gene.[5–15] However, the acquisition of an additional mutation (T790M) in exon 20 of *EGFR* results in the development of resistance to EGFR-TKI.[16–19] Irreversible EGFR-TKI are thought to be a potential therapeutic option for overcoming such resistance.[20,21] Amplification of the gene for the receptor tyrosine kinase MET has also recently been identified as a mechanism of gefitinib resistance, being detected in 22% of tumor samples from NSCLC patients with *EGFR* mutations who acquired gefitinib resistance.[22,23] Exposure of gefitinib-resistant NSCLC cells with *MET* amplification to the MET-TKI PHA-665752 or to gefitinib alone did not inhibit cell growth or survival signaling, given that both EGFR and MET signaling were found to be activated and to be mediated by ErbB3 (also known as Her3) in these cells.[22,23] However, the combination of gefitinib and PHA-665752 overcame gefitinib resistance attributable to *MET* amplification.[22,23] No single agent that overcomes such resistance has been identified to date.

The proto-oncogene *SRC* has been implicated in the development and poor clinical prognosis of several types of solid tumor as a result of the mediation by its product of signaling between integrins or receptor tyrosine kinases and their downstream effectors.[24–26] We have examined the potential role of Src in EGFR or MET signaling and whether Src inhibitors might block these signaling pathways in gefitinib-resistant NSCLC cells with *MET* amplification. We also evaluated the potential antitumor effect of Src inhibitors in order to provide insight into the mechanism by which such inhibitors might overcome gefitinib resistance in NSCLC cells with *MET* amplification.

Materials and Methods

Cell lines and reagents. The human NSCLC cell lines H1299, H460, HCC827, HCC827 GR5, HCC827 GR6, and PC9 were obtained as described previously.[22,27] H1838 and H820 cells were obtained from the American Type Culture Collection (Manassas, VA, USA). EBC-1 cells were obtained from the Health Science Research Resources Bank (Tokyo, Japan). PC9/ZD cells were established as a gefitinib-resistant clone from PC9 cells as previously described[28] and were shown to harbor the T790M mutation of *EGFR* by both PCR invader and PCR clamp assays carried out as previously described.[29,30] HCC827, PC9, and PC9/ZD cells were cultured under a humidified atmosphere of 5% CO_2 at 37°C in RPMI-1640 medium (Sigma, St Louis, MO, USA) supplemented with 10% FBS. HCC827 GR5 and HCC827 GR6 cells were cultured in RPMI-1640 medium supplemented with 10% FBS and 1 μM gefitinib. Dasatinib was kindly provided by Bristol-Myers Squibb (New York, NY, USA), gefitinib was obtained from AstraZeneca (Macclesfield, UK), PP1 was from Biomol Research Laboratories (Plymouth Meeting, PA, USA), and PHA-665752 was from Tocris Bioscience (Bristol, UK).

[6]To whom correspondence should be addressed.
E-mail: chi-okamoto@dotd.med.kindai.ac.jp

doi: 10.1111/j.1349-7006.2009.01368.x

Immunoblot analysis. Immunoblot analysis was carried out as described previously.[27] Antibodies to the Y845-phosphorylated form of EGFR, to EGFR, to phosphorylated Erk, to Erk, to phosphorylated Akt, to Akt, and to β-actin as well as HRP-conjugated goat antibodies to mouse or rabbit IgG were obtained as described previously.[27] Antibodies to the Y1234/Y1235-phosphorylated form of MET, to the Y1289-phosphorylated form of ErbB3, to the Y416-phosphorylated form of Src, to Src, and to PARP were obtained from Cell Signaling Technology (Beverly, MA, USA). Antibodies to MET were from Zymed (South San Francisco, CA, USA) and those to ErbB3 were from Santa Cruz Biotechnology (Santa Cruz, CA, USA).

Immunoprecipitation assay. Total cell lysates (500 μg protein) were incubated overnight at 4°C with 5 μg of a mouse monoclonal antibody (H-12) to total Src (Santa Cruz Biotechnology) in a final volume of 200 μL. The immune complexes were precipitated by further incubation for 2 h at 4°C with a suspension of protein G- and protein A-conjugated agarose (Calbiochem, Darmstadt, Germany). The immunoprecipitates were resolved by SDS-PAGE on a 7.5% gel, and the separated proteins were subjected to immunoblot analysis as described previously,[27] with the exception that the incubation with primary antibodies was carried out for 48 h.

Cell growth inhibition assay. Cells were plated in 96-well flat-bottomed plates and cultured for 24 h before exposure to various concentrations of tested drugs for 72 h. TetraColor One (5 mM tetrazolium monosodium salt and 0.2 mM 1-methoxy-5-methyl phenazinium methylsulfate; Seikagaku, Tokyo, Japan) was then added to each well, and the cells were incubated for 3 h at 37°C before measurement of absorbance at 490 nm with a Multiskan Spectrum instrument (Thermo Labsystems, Boston, MA, USA). Absorbance values were expressed as a percentage of that for untreated cells.

Assessment of tumor growth inhibition *in vivo*. Tumor cells (2×10^6) were injected s.c. into the right hind leg of 7-week-old female athymic nude mice. The mice were divided into three treatment groups of five animals: those treated over 28 days by oral gavage daily of vehicle, gefitinib (50 mg/kg), or dasatinib (15 mg/kg). Treatment was initiated when tumors in each group achieved an average volume of 200 mm^3, with tumor volume being determined twice weekly after the onset of treatment from caliper measurement of tumor length (L) and width (W) according to the formula $LW^2/2$.

Statistical analysis. Data are presented as means ± SE as indicated and were analyzed by Student's t-test. A P-value of <0.05 was considered statistically significant.

Results

Src is activated in gefitinib-resistant NSCLC cells with *MET* amplification. Amplification of *MET* is one mechanism for the acquisition of resistance to EGFR-TKI in NSCLC.[22,23] To explore approaches that might overcome such resistance, we examined the activation status of several signaling molecules in sublines of the gefitinib-sensitive, *EGFR* mutation-positive human NSCLC cell line HCC827 that have acquired *MET* amplification and gefitinib resistance. Immunoblot analysis revealed that the level of phosphorylation (activation) of both MET and ErbB3 was markedly increased in the HCC827 GR5 and GR6 sublines compared with the parental HCC827 cells (Fig. 1A), consistent with previous observations.[22,23] Furthermore, we found that the level of Src activation was also markedly increased in HCC827 GR cells compared with HCC827 cells (Fig. 1A). Such Src activation was not observed in PC9/ZD cells (Fig. 1A), a subline of the gefitinib-sensitive, *EGFR* mutation-positive human NSCLC cell line PC9 that has acquired a secondary T790M mutation of *EGFR* and consequent gefitinib resistance. These results thus suggested that Src might contribute to gefitinib resistance in NSCLC cells with *MET* amplification. We also found that H1838, EBC-1, and H820 NSCLC cells with *MET* amplification[31–33] have higher activation of Src than that in NSCLC cells without *MET* amplification (H1299 and H460) (Fig. 1B). These results suggested that Src activation is associated with *MET* amplification in NSCLC cells.

Src activation blocked by a MET inhibitor in gefitinib-resistant NSCLC cells with *MET* amplification. Src associates with many receptor tyrosine kinases including EGFR and MET and transduces signals to a variety of downstream effectors of these receptors.[24–26,34–36] To examine whether Src participates in MET or EGFR signaling in cells with *EGFR* mutations and with or without *MET* amplification, we examined the effects of the MET inhibitor PHA-665752 or the EGFR-TKI gefitinib on Src

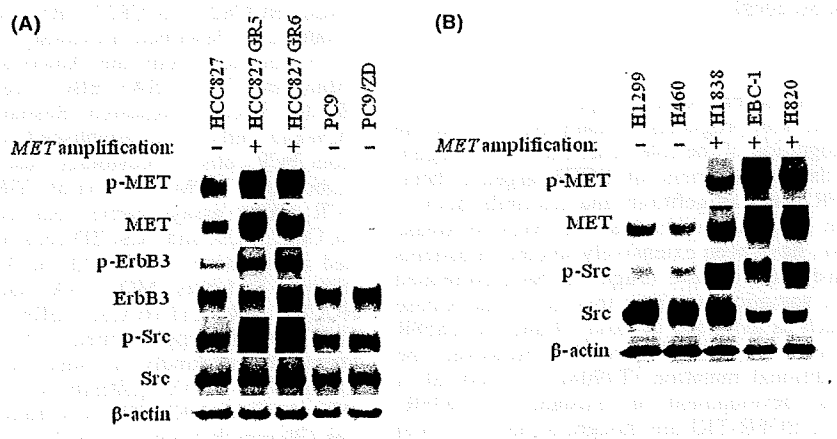

Fig. 1. Activation of Src in non-small cell lung cancer cells with or without *MET* amplification. (A) HCC827 cells, their gefitinib-resistant clones with *MET* amplification (HCC827 GR5 and GR6), PC9 cells, and their gefitinib-resistant clone with a secondary T790M mutation of epidermal growth factor receptor (PC9/ZD) were incubated for 24 h in medium containing 10% serum. Cell lysates were then prepared and subjected to immunoblot analysis with antibodies to phosphorylated (p-) or total forms of MET, ErbB3, and Src as well as with those to β-actin (loading control). (B) H1299 and H460 cells without *MET* amplification, and H1838, EBC-1, and H820 cells with *MET* amplification were incubated for 24 h in medium containing 10% serum. Cell lysates were then prepared and subjected to immunoblot analysis with antibodies to phosphorylated (p-) or total forms of MET and Src as well as with those to β-actin (loading control).

doi: 10.1111/j.1349-7006.2009.01368.x

activation in HCC827 and HCC827 GR cells. In the parental HCC827 cells, Src activity (phosphorylation) was reduced by PHA-665752 and was abolished by gefitinib (Fig. 2A). In contrast, Src activation was partially reduced by PHA-665752 and was inhibited to a much lesser extent by gefitinib in HCC827 GR5 cells (Fig. 2A). Combined treatment with gefitinib and PHA-665752 resulted in complete suppression of Src activation in both the parental and GR cells (Fig. 2A). These results suggested that Src activation is dependent on MET signaling to a greater extent than on EGFR signaling in gefitinib-resistant cells with *MET* amplification, whereas the opposite is the case for cells without *MET* amplification.

Effects of Src inhibitors on EGFR, ErbB3, and MET activation in gefitinib-resistant NSCLC cells with *MET* amplification. Src activates EGFR by phosphorylating the Y845 residue of the receptor,[37] and it also interacts with MET.[35] We therefore examined the effects of the Src inhibitors PP1 and dasatinib on EGFR, ErbB3, and MET activation. Both PP1 and dasatinib abolished EGFR activation and inhibited ErbB3 and MET activation in parental HCC827 cells (Fig. 2A). In contrast, these Src inhibitors did not suppress ErbB3 or MET activation and induced only partial inhibition of EGFR activation in HCC827 GR5 cells (Fig. 2A), suggesting that *MET* amplification affects the interactions of EGFR, ErbB3, and MET with Src.

Increased association between MET and Src in gefitinib-resistant NSCLC cells with *MET* amplification. We examined the effects of *MET* amplification on the physical association of Src with EGFR, MET, and ErbB3. Src was immunoprecipitated from both HCC827 and HCC827 GR5 cell lysates, and the resulting precipitates were subjected to immunoblot analysis with antibodies to EGFR, MET, ErbB3, or Src. The amount of MET associated with Src was greater for HCC827 GR5 cells than for HCC827 cells, whereas the amount of EGFR associated with Src was greater for HCC827 cells than for HCC827 GR5 cells (Fig. 2B). No association of ErbB3 with Src was apparent for either cell type. These results suggested that *MET* amplification results in an increase in the association between MET and Src, as well as a concomitant decrease in that between EGFR and Src, in HCC827 GR cells.

Src inhibitors block Akt and Erk signaling in gefitinib-resistant NSCLC cells with *MET* amplification. We next examined the effects of the Src inhibitors PP1 and dasatinib on Akt and Erk signaling pathways, both of which are activated by EGFR and MET. Both PP1 and dasatinib induced complete inhibition of Akt and Erk activation, as did gefitinib, in the parental HCC827 cells (Fig. 2A). Consistent with previous observations,[22,23] the combination of gefitinib and PHA-665752 inhibited Akt and Erk activation in HCC827 GR5 cells, whereas neither agent alone had such an effect (Fig. 2A). Both PP1 and dasatinib inhibited Akt and Erk activation to similar extents as the combination of gefitinib and PHA-665752 in HCC827 GR5 cells (Fig. 2A). A single agent (Src inhibitor) was thus sufficient to block Akt and Erk signaling, which is important for cell survival and proliferation, respectively, in gefitinib-resistant NSCLC cells with *MET* amplification.

Src inhibitor dasatinib suppresses growth of gefitinib-resistant NSCLC cells with *MET* amplification. The combination of gefitinib and PHA-665752 was recently shown to inhibit the growth of, and to induce apoptosis in, HCC827 GR cells with *MET* amplification, whereas neither agent alone had such an effect.[22,23] Given that we found that Src inhibitors block Akt and Erk signaling pathways as effectively as the combination of gefitinib and PHA-665752 in such cells, we examined whether dasatinib might overcome gefitinib resistance in HCC827 GR cells. In the parental HCC827 cells, both gefitinib and dasatinib as well as the combination of gefitinib and PHA-665752 effectively inhibited cell growth, but PHA-665752 alone had less inhibitory effect (Fig. 3A). Dasatinib inhibited cell growth in a concentration-dependent manner by the same marked extent as the combination of gefitinib and PHA-665752, even in HCC827 GR5 cells, whereas neither gefitinib nor PHA-665752 alone had a substantial effect (Fig. 3B). We also examined the effect of dasatinib on apoptosis as assessed on the basis of cleavage of the enzyme PARP in both HCC827 and HCC827 GR5 cells. Dasatinib (but not gefitinib) induced apoptosis in HCC827 GR5 cells to the same marked extent as did the combination of gefitinib and PHA-665752, whereas dasatinib and gefitinib each induced apoptosis in the parental HCC827 cells (Fig. 3C). These results suggested that Src inhibitors efficiently induce growth inhibition and apoptosis in gefitinib-resistant NSCLC cells with *MET* amplification.

Src inhibitor dasatinib inhibits tumor growth in gefitinib-resistant NSCLC xenografts with *MET* amplification. To determine whether the efficacy of dasatinib in gefitinib-resistant NSCLC cells with *MET* amplification observed *in vitro* might also be apparent *in vivo*, we examined the antitumor effects of dasatinib in nude mice with solid tumors formed by HCC827 GR5 cells injected into the right hind leg. Gefitinib (50 mg/kg)

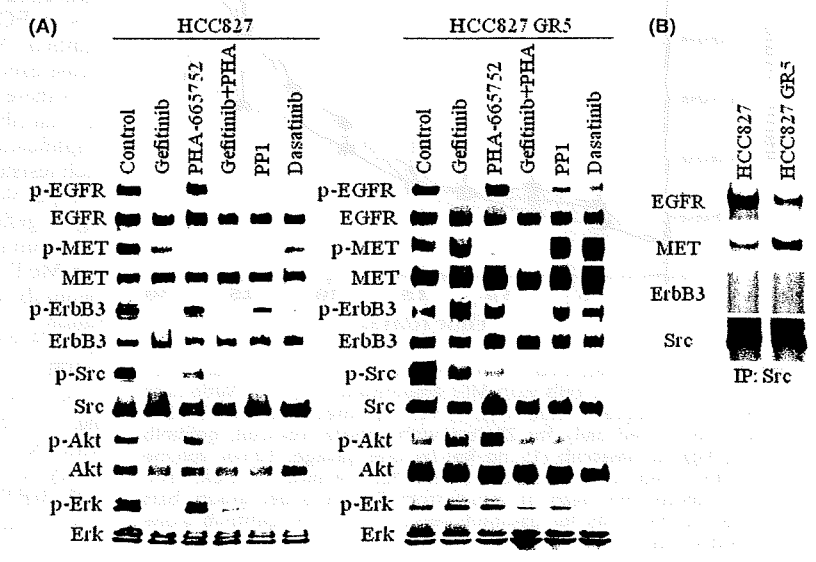

Fig. 2. Effects of various inhibitors on epidermal growth factor receptor (EGFR) and MET signaling in gefitinib-resistant non-small cell lung cancer cells with *MET* amplification. (A) HCC827 cells and a gefitinib-resistant clone with *MET* amplification (HCC827 GR5) were incubated for 12 h in the absence (control) or presence of gefitinib alone (1 μM), PHA-665752 alone (1 μM), gefitinib and PHA-665752 combined, PP1 (10 μM), or dasatinib (500 nM) in medium containing 10% serum. Cell lysates were then subjected to immunoblot analysis with antibodies to phosphorylated (p-) or total forms of EGFR, MET, ErbB3, Src, Akt, and Erk. (B) HCC827 and HCC827 GR5 cells were incubated for 24 h in medium containing 10% serum, lysed, and subjected to immunoprecipitation (IP) with an antibody to Src. The resulting precipitates were subjected to immunoblot analysis with antibodies to EGFR, MET, ErbB3, and Src.

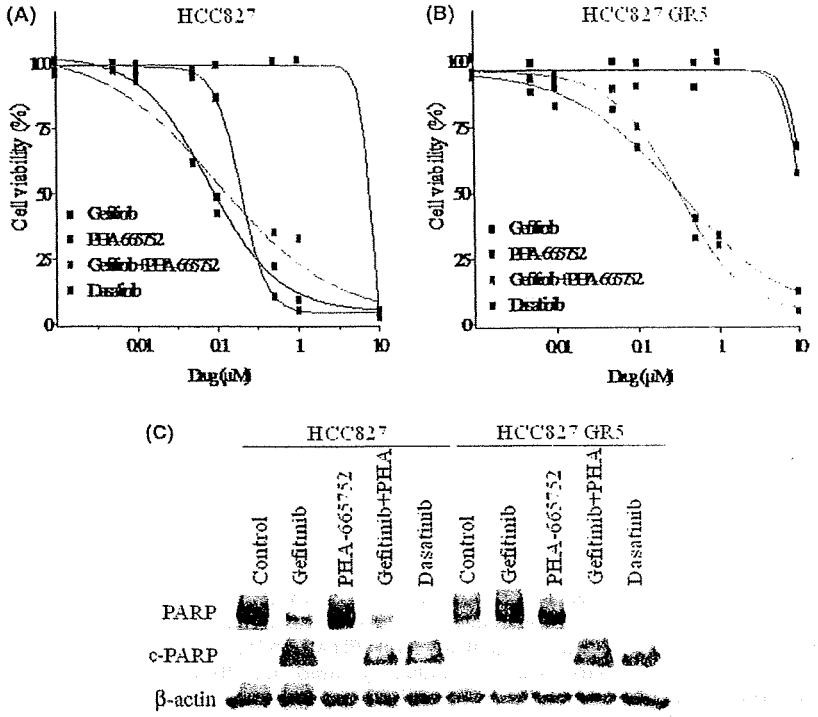

Fig. 3. Effects of dasatinib on growth and apoptosis in gefitinib-resistant non-small cell lung cancer cells with *MET* amplification. (A) HCC827 cells or (B) HCC827 GR5 cells were treated for 72 h with increasing concentrations of gefitinib alone, PHA-665752 alone, gefitinib and PHA-665752 in combination, or dasatinib alone in medium containing 10% serum, after which cell viability was assessed. Data are means of triplicates from a representative experiment and are expressed as a percentage of the value for untreated cells. (C) HCC827 and HCC827 GR5 cells were incubated for 72 h with gefitinib (1 μM) alone, PHA-665752 (1 μM) alone, gefitinib plus PHA-665752, or dasatinib (1 μM) in medium containing 10% serum. Cell lysates were then prepared and subjected to immunoblot analysis with antibodies to poly(ADP-ribose) polymerase (PARP) and to β-actin. The positions of intact PARP (116 kDa) and the 85-kDa cleavage fragment (c-PARP) are shown.

could not reduce tumor size compared with vehicle treatment (Fig. 4). In contrast, dasatinib (15 mg/kg) inhibited tumor growth in HCC827 GR5 xenografts to a significantly greater extent than did treatment with gefitinib or vehicle alone (Fig. 4). These results indicated that Src inhibitor effectively exerts antitumor effects in gefitinib-resistant NSCLC xenografts with *MET* amplification.

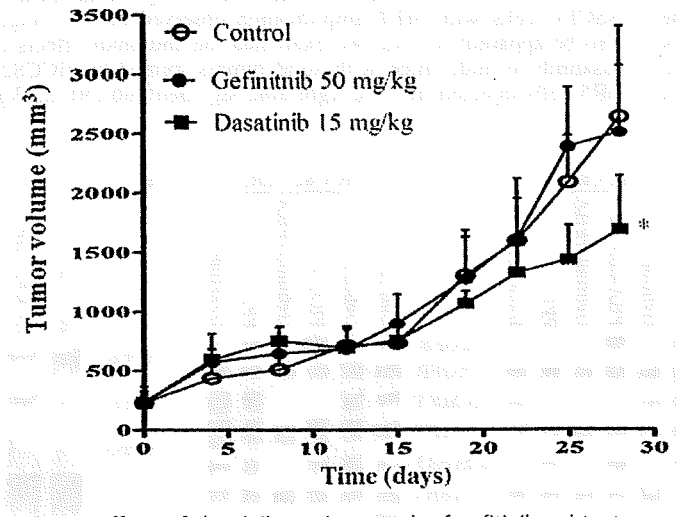

Fig. 4. Effects of dasatinib on the growth of gefitinib-resistant non-small cell lung cancer cells with *MET* amplification *in vivo*. Nude mice with tumor xenografts established by s.c. implantation of HCC827 GR5 cells were treated daily for 28 days with vehicle (control), gefitinib (50 mg/kg), or dasatinib (15 mg/kg) by oral gavage. Tumor volume was determined at the indicated times after the onset of treatment. Points indicate the mean of values from five mice per group; bars indicate SE. *$P < 0.05$ for dasatinib *versus* control or gefitinib alone (Student's *t*-test).

Discussion

The emergence of *MET* amplification induces ErbB3-dependent downstream signaling mediated by Akt and Erk that is important for cell survival and proliferation, ultimately leading to the development of gefitinib resistance, in NSCLC cells with *EGFR* mutations.[22,23] Although the combination of the specific MET inhibitor PHA-665752 and gefitinib is considered promising for overcoming gefitinib resistance due to *MET* amplification, a single-agent therapy to overcome such resistance would be more desirable.[22,23] We have shown that, in addition to MET activation, Src is markedly activated in NSCLC cells with *MET* amplification, including HCC827 GR cells. Forced expression of Src has previously been shown to result in gefitinib resistance in gallbladder adenocarcinoma cells[38] and to promote tumorigenesis in EGFR-overexpressing mammary epithelial cells.[39] In addition, MET and Src cooperate to mediate proliferation of breast cancer cells in the presence of EGFR-TKI.[34] Consistent with these previous observations, our results now suggest that Src contributes to gefitinib resistance in NSCLC cells with *MET* amplification and is a potential target molecule for overcoming such resistance.

To explore how Src activation affects MET or EGFR signaling in gefitinib-resistant NSCLC cells with *MET* amplification, we examined the effects of Src inhibitors on EGFR, ErbB3, and MET activation in both HCC827 and HCC827 GR5 cells. Gefitinib was previously shown to inhibit ErbB3 and MET activation as well as EGFR activation in the parental HCC827 cells,[22,23,40] suggestive of a functional interaction between EGFR and both ErbB3 and MET in *EGFR*-mutant NSCLC cells without *MET* amplification (Fig. 5A). In contrast, gefitinib did not inhibit ErbB3 or MET activation in HCC827 GR cells, with the combination of gefitinib and PHA-665752 being necessary to achieve inhibition of ErbB3 activation in these cells with *MET* amplification.[22,23] In addition, endogenous ErbB3 was co-immunoprecipitated with MET from HCC827 GR cells

doi: 10.1111/j.1349-7006.2009.01368.x

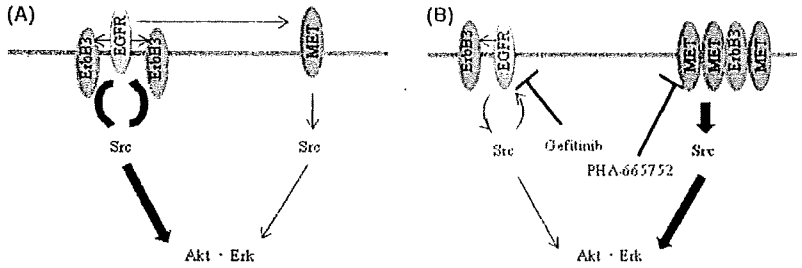

Fig. 5. Models for signaling pathways in gefitinib-sensitive non-small cell lung cancer (NSCLC) cells (A) and gefitinib-resistant NSCLC cells with acquired *MET* amplification (B). Src functions downstream of both epidermal growth factor receptor (EGFR) and MET as well as upstream of Akt and Erk signaling pathways and EGFR. However, the dependency of Src signaling is shifted from EGFR to MET and MET associates with ErbB3 after the acquisition of *MET* amplification. EGFR mediates, at least in part, activation of MET in gefitinib-sensitive NSCLC cells, whereas EGFR and MET function independently of each other in gefitinib-resistant NSCLC cells with acquired *MET* amplification. Pathways targeted by gefitinib or PHA-665752 are indicated, and the relative activities of signaling pathways are denoted by the width of the arrows.

but not from HCC827 cells.[22,23] These previous results thus suggested that ErbB3 signaling becomes more dependent on MET than on EGFR after emergence of *MET* amplification, and that the MET-ErbB3 signaling complex is largely independent of EGFR signaling (Fig. 5B).[22,23] We have shown that Src inhibitors reduced the extent of EGFR activation in both HCC827 and HCC827 GR5 cells, consistent with previous observations showing that Src mediates EGFR activation by phosphorylating its Y845 residue.[37,41] In HCC827 GR5 cells, however, Src inhibitors did not inhibit ErbB3 or MET activation, despite it doing so in the parental HCC827 cells. These results support the notion that MET signaling is independent of EGFR signaling as a result of the shift of the dependence of ErbB3 signaling from EGFR to MET in HCC827 GR cells (Fig. 5B).[22,23]

We examined whether *MET* amplification affects the physical association between Src and either EGFR, MET, or ErbB3 by immunoprecipitation. The association between MET and Src was increased in HCC827 GR5 cells compared with that in HCC827 cells, whereas the association between EGFR and Src was reduced in HCC827 GR5 cells. These findings are consistent with our results showing that PHA-665752 blocks Src activation to a greater extent in HCC827 GR5 cells than in HCC827 cells, a pattern opposite to that for the effects of gefitinib (Fig. 5). The mechanism of increased association between MET and Src induced by acquired *MET* amplification has remained unclear. It is possible that *MET* amplification alters the protein expression which mediates binding of Src to MET. On the basis of the notion that Src is activated downstream of MET signaling in HCC827 GR cells, we examined the effects of Src inhibitors in these cells on Akt and Erk signaling pathways, both of which are known to be activated by Src.[24–26,42] We have shown that Src inhibitors markedly inhibited Akt and Erk signaling pathways in gefitinib-resistant NSCLC cells with *MET* amplification. Previous studies found that neither gefitinib nor PHA-665752 alone blocked Akt or Erk pathways in HCC827 GR cells,[22,23] with the combination of both of these agents being necessary for such inhibition, consistent with the notion that Akt and Erk pathways are dependent on both EGFR and MET signaling in these cells (Fig. 5B). We observed that gefitinib and PHA-665752 each induced a slight increase in the phosphorylation levels of Akt in HCC827 GR5 cells (Fig. 2A), possibly because EGFR and MET pathways functionally compensate for each other when either is inhibited. Our results suggest that Src functions downstream of both EGFR and MET, but that it is mainly dependent on MET signaling in HCC827 GR cells. Together, our observations explain the ability of Src inhibitors to suppress Akt and Erk activation in gefitinib-resistant NSCLC cells with *MET* amplification (Fig. 5B).

Finally, we found that Src inhibitor dasatinib also inhibited the growth of HCC827 GR5 cells as well as did combined treatment with gefitinib and PHA-665752. HCC827 GR5 cells underwent apoptosis, as detected by PARP cleavage, after treatment with dasatinib. Furthermore, dasatinib inhibited tumor growth in HCC827 GR5 xenografts to a significantly greater extent than treatment with gefitinib alone. Our present data suggest that Src inhibitors might overcome gefitinib resistance in NSCLC patients with *MET* amplification. Our findings strengthen the rationale of the ongoing clinical trial of dasatinib for NSCLC patients who no longer respond to erlotinib or gefitinib (http://www.clinicaltrials.gov). The results of this clinical trial should provide insight into the relation between the efficacy of Src inhibitors and whether gefitinib resistance is attributable to the secondary T790M mutation of *EGFR* or to acquired *MET* amplification.

Abbreviations

EGFR	epidermal growth factor receptor
NSCLC	non-small cell lung cancer
PARP	poly(ADP-ribose) polymerase
TKI	tyrosine kinase inhibitor

References

1 Gullick WJ. Prevalence of aberrant expression of the epidermal growth factor receptor in human cancers. *Br Med Bull* 1991; 47: 87–98.
2 Salomon DS, Brandt R, Ciardiello F, Normanno N. Epidermal growth factor-related peptides and their receptors in human malignancies. *Crit Rev Oncol Hematol* 1995; 19: 183–232.
3 Harari PM. Epidermal growth factor receptor inhibition strategies in oncology. *Endocr Relat Cancer* 2004; 11: 689–708.
4 Ettinger DS. Clinical implications of EGFR expression in the development and progression of solid tumors: focus on non-small cell lung cancer. *Oncologist* 2006; 11: 358–73.
5 Lynch TJ, Bell DW, Sordella R *et al.* Activating mutations in the epidermal growth factor receptor underlying responsiveness of non-small-cell lung cancer to gefitinib. *N Engl J Med* 2004; 350: 2129–39.
6 Paez JG, Janne PA, Lee JC *et al.* EGFR mutations in lung cancer: correlation with clinical response to gefitinib therapy. *Science* 2004; 304: 1497–500.
7 Pao W, Miller V, Zakowski M *et al.* EGF receptor gene mutations are common in lung cancers from "never smokers" and are associated with sensitivity of tumors to gefitinib and erlotinib. *Proc Natl Acad Sci U S A* 2004; 101: 13306–11.
8 Mitsudomi T, Kosaka T, Endoh H *et al.* Mutations of the epidermal growth factor receptor gene predict prolonged survival after gefitinib treatment in

patients with non-small-cell lung cancer with postoperative recurrence. *J Clin Oncol* 2005; **23**: 2513–20.
9 Takano T, Ohe Y, Sakamoto H *et al.* Epidermal growth factor receptor gene mutations and increased copy numbers predict gefitinib sensitivity in patients with recurrent non-small-cell lung cancer. *J Clin Oncol* 2005; **23**: 6829–37.
10 Han SW, Kim TY, Hwang PG *et al.* Predictive and prognostic impact of epidermal growth factor receptor mutation in non-small-cell lung cancer patients treated with gefitinib. *J Clin Oncol* 2005; **23**: 2493–501.
11 Tsao MS, Sakurada A, Cutz JC *et al.* Erlotinib in lung cancer – molecular and clinical predictors of outcome. *N Engl J Med* 2005; **353**: 133–44.
12 Kosaka T, Yatabe Y, Endoh H, Kuwano H, Takahashi T, Mitsudomi T. Mutations of the epidermal growth factor receptor gene in lung cancer: biological and clinical implications. *Cancer Res* 2004; **64**: 8919–23.
13 Shigematsu H, Lin L, Takahashi T *et al.* Clinical and biological features associated with epidermal growth factor receptor gene mutations in lung cancers. *J Natl Cancer Inst* 2005; **97**: 339–46.
14 Tokumo M, Toyooka S, Kiura K *et al.* The relationship between epidermal growth factor receptor mutations and clinicopathologic features in non-small cell lung cancers. *Clin Cancer Res* 2005; **11**: 1167–73.
15 Sharma SV, Bell DW, Settleman J, Haber DA. Epidermal growth factor receptor mutations in lung cancer. *Nat Rev Cancer* 2007; **7**: 169–81.
16 Kobayashi S, Boggon TJ, Dayaram T *et al.* EGFR mutation and resistance of non-small-cell lung cancer to gefitinib. *N Engl J Med* 2005; **352**: 786–92.
17 Pao W, Miller VA, Politi KA *et al.* Acquired resistance of lung adenocarcinomas to gefitinib or erlotinib is associated with a second mutation in the EGFR kinase domain. *PLoS Med* 2005; **2**: e73.
18 Kosaka T, Yatabe Y, Endoh H *et al.* Analysis of epidermal growth factor receptor gene mutation in patients with non-small cell lung cancer and acquired resistance to gefitinib. *Clin Cancer Res* 2006; **12**: 5764–9.
19 Yun CH, Mengwasser KE, Toms AV *et al.* The T790M mutation in EGFR kinase causes drug resistance by increasing the affinity for ATP. *Proc Natl Acad Sci U S A* 2008; **105**: 2070–5.
20 Kwak EL, Sordella R, Bell DW *et al.* Irreversible inhibitors of the EGF receptor may circumvent acquired resistance to gefitinib. *Proc Natl Acad Sci U S A* 2005; **102**: 7665–70.
21 Engelman JA, Mukohara T, Zejnullahu K *et al.* Allelic dilution obscures detection of a biologically significant resistance mutation in EGFR-amplified lung cancer. *J Clin Invest* 2006; **116**: 2695–706.
22 Engelman JA, Zejnullahu K, Mitsudomi T *et al.* MET amplification leads to gefitinib resistance in lung cancer by activating ERBB3 signaling. *Science* 2007; **316**: 1039–43.
23 Arteaga CL. HER3 and mutant EGFR meet MET. *Nat Med* 2007; **13**: 675–7.
24 Alvarez RH, Kantarjian HM, Cortes JE. The role of Src in solid and hematologic malignancies: development of new-generation Src inhibitors. *Cancer* 2006; **107**: 1918–29.
25 Summy JM, Gallick GE. Src family kinases in tumor progression and metastasis. *Cancer Metastasis Rev* 2003; **22**: 337–58.
26 Summy JM, Gallick GE. Treatment for advanced tumors: SRC reclaims center stage. *Clin Cancer Res* 2006; **12**: 1398–401.
27 Okabe T, Okamoto I, Tamura K *et al.* Differential constitutive activation of the epidermal growth factor receptor in non-small cell lung cancer cells bearing EGFR gene mutation and amplification. *Cancer Res* 2007; **67**: 2046–53.
28 Koizumi F, Shimoyama T, Taguchi F, Saijo N, Nishio K. Establishment of a human non-small cell lung cancer cell line resistant to gefitinib. *Int J Cancer* 2005; **116**: 36–44.
29 Tadokoro K, Kobayashi M, Yamaguchi T *et al.* Classification of hepatitis B virus genotypes by the PCR-Invader method with genotype-specific probes. *J Virol Methods* 2006; **138**: 30–9.
30 Nagai Y, Miyazawa H, Huqun *et al.* Genetic heterogeneity of the epidermal growth factor receptor in non-small cell lung cancer cell lines revealed by a rapid and sensitive detection system, the peptide nucleic acid-locked nucleic acid PCR clamp. *Cancer Res* 2005; **65**: 7276–82.
31 Jagadeeswaran R, Surawska H, Krishnaswamy S *et al.* Paxillin is a target for somatic mutations in lung cancer: implications for cell growth and invasion. *Cancer Res* 2008; **68**: 132–42.
32 Lutterbach B, Zeng Q, Davis LJ *et al.* Lung cancer cell lines harboring MET gene amplification are dependent on Met for growth and survival. *Cancer Res* 2007; **67**: 2081–8.
33 Bean J, Brennan C, Shih JY *et al.* MET amplification occurs with or without T790M mutations in EGFR mutant lung tumors with acquired resistance to gefitinib or erlotinib. *Proc Natl Acad Sci U S A* 2007; **104**: 20932–7.
34 Mueller KL, Hunter LA, Ethier SP, Boerner JL. Met and c-Src cooperate to compensate for loss of epidermal growth factor receptor kinase activity in breast cancer cells. *Cancer Res* 2008; **68**: 3314–22.
35 Bolanos-Garcia VM. MET meet adaptors: functional and structural implications in downstream signalling mediated by the Met receptor. *Mol Cell Biochem* 2005; **276**: 149–57.
36 Mao W, Irby R, Coppola D *et al.* Activation of c-Src by receptor tyrosine kinases in human colon cancer cells with high metastatic potential. *Oncogene* 1997; **15**: 3083–90.
37 Sato K, Sato A, Aoto M, Fukami Y. c-Src phosphorylates epidermal growth factor receptor on tyrosine 845. *Biochem Biophys Res Commun* 1995; **215**: 1078–87.
38 Qin B, Ariyama H, Baba E *et al.* Activated Src and Ras induce gefitinib resistance by activation of signaling pathways downstream of epidermal growth factor receptor in human gallbladder adenocarcinoma cells. *Cancer Chemother Pharmacol* 2006; **58**: 577–84.
39 Dimri M, Naramura M, Duan L *et al.* Modeling breast cancer-associated c-Src and EGFR overexpression in human MECs: c-Src and EGFR cooperatively promote aberrant three-dimensional acinar structure and invasive behavior. *Cancer Res* 2007; **67**: 4164–72.
40 Guo A, Villen J, Kornhauser J *et al.* Signaling networks assembled by oncogenic EGFR and c-Met. *Proc Natl Acad Sci U S A* 2008; **105**: 692–7.
41 Zhang J, Kalyankrishna S, Wislez M *et al.* SRC-family kinases are activated in non-small cell lung cancer and promote the survival of epidermal growth factor receptor-dependent cell lines. *Am J Pathol* 2007; **170**: 366–76.
42 Song L, Morris M, Bagui T, Lee FY, Jove R, Haura EB. Dasatinib (BMS-354825) selectively induces apoptosis in lung cancer cells dependent on epidermal growth factor receptor signaling for survival. *Cancer Res* 2006; **66**: 5542–8.

doi: 10.1111/j.1349-7006.2009.01368.x

Inhibition of Insulin-Like Growth Factor 1 Receptor by CP-751,871 Radiosensitizes Non–Small Cell Lung Cancer Cells

Tsutomu Iwasa,[1] Isamu Okamoto,[1] Minoru Suzuki,[2] Erina Hatashita,[1] Yuki Yamada,[1] Masahiro Fukuoka,[3] Koji Ono,[2] and Kazuhiko Nakagawa[1]

Abstract

Purpose: Therapeutic strategies that target the insulin-like growth factor I receptor (IGF-1R) hold promise for a wide variety of cancers. We have now investigated the effect of CP-751,871, a fully human monoclonal antibody specific for IGF-IR, on the sensitivity of human non–small cell lung cancer (NSCLC) cell lines to radiation.

Experimental Design: The radiosensitizing effect of CP-751,871 was evaluated on the basis of cell death, clonogenic survival, and progression of tumor xenografts. Radiation-induced damage was evaluated by immunofluorescence analysis of the histone γ-H2AX and Rad51.

Results: A clonogenic survival assay revealed that CP-751,871 increased the sensitivity of NSCLC cells to radiation *in vitro*. CP-751,871 inhibited radiation-induced IGF-IR signaling, and potentiated the radiation-induced increases both in the number of apoptotic cells and in the activity of caspase-3. Immunofluorescence analysis of the histone γ-H2AX and Rad51 also showed that CP-751,871 inhibited the repair of radiation-induced DNA double-strand breaks. Finally, combination therapy with CP-751,871 and radiation delayed the growth of NSCLC tumor xenografts in nude mice to a greater extent than did either treatment modality alone.

Conclusions: These results show that CP-751,871 sensitizes NSCLC cells to radiation both *in vitro* and *in vivo*, and that this effect of CP-751,871 is likely attributable to the inhibition of DNA repair and enhancement of apoptosis that result from attenuation of IGF-IR signaling. Combined treatment with CP-751,871 and radiation thus warrants further investigation in clinical trials as a potential anticancer strategy. (Clin Cancer Res 2009;15(16):5117–25)

The insulin-like growth factor I receptor (IGF-IR) is a receptor tyrosine kinase that contributes to the regulation of cell growth, transformation, and apoptosis, and plays an important role in tumor cell proliferation and survival (1, 2). Antisense oligonucleotides, inhibitory peptides, and kinase inhibitors that target IGF-IR, as well as dominant negative mutant and soluble forms of the receptor have been found to inhibit the proliferation of tumor cell lines *in vitro* and in experimental mouse models (3–7). Targeting of IGF-IR is thus a promising strategy for cancer therapy. The two most investigated therapeutic approaches in preclinical models are based on specific tyrosine kinase inhibitors and monoclonal antibodies (mAb; ref. 7–11). Although IGF-IR tyrosine kinase inhibitors have a high affinity for IGF-IR, cross-inhibition of the insulin receptor remains a problem because of the high level of sequence similarity between the tyrosine kinase domains of these two receptors (12). Such cross-inhibition has the potential to induce symptoms of diabetes in treated individuals (13). In contrast, antibodies that target the extracellular domain of IGF-IR are highly selective for IGF-IR. Currently available antibodies to IGF-IR are of the IgG1 and IgG2 isotypes (7–10). These two isotypes differ in that IgG2 antibodies manifest a longer half-life in humans, whereas IgG1 antibodies are more effective at eliciting immune cell effector functions (antibody-dependent cytotoxicity). CP-751,871 is a potent, fully human IgG2 mAb specific for IGF-IR that inhibits tumor growth as a single agent and enhances the efficacy of other anticancer agents in human tumor xenograft models (10). CP-751,871 is thus an attractive candidate drug for cancer therapy, and clinical trials of this agent in combination with chemotherapy are currently underway for certain types of cancer.

Overexpression of IGF-IR in NIH 3T3 fibroblasts confers radioresistance in preclinical models (14). Expression and activation of IGF-IR have also been associated with resistance to

[1]Department of Medical Oncology, Kinki University School of Medicine, Osaka-Sayama, Osaka, Japan; [2]Radiation Oncology Research Laboratory, Research Reactor Institute, Kyoto University, Sennan-gun, Osaka, Japan; and [3]Department of Medical Oncology, Kinki University School of Medicine, Sakai Hospital, Sakai, Osaka, Japan

Received 2/24/09; revised 4/30/09; accepted 5/18/09; published OnlineFirst 8/11/09.

The costs of publication of this article were defrayed in part by the payment of page charges. This article must therefore be hereby marked *advertisement* in accordance with 18 U.S.C. Section 1734 solely to indicate this fact.

Note: Supplementary data for this article are available at Clinical Cancer Research Online (http://clincancerres.aacrjournals.org/).

Requests for reprints: Isamu Okamoto, Department of Medical Oncology, Kinki University School of Medicine, 377-2 Ohno-higashi, Osaka-Sayama, Osaka 589-8511, Japan. Phone: 81-72-366-0221; Fax: 81-72-360-5000; E-mail: chi-okamoto@dotd.med.kindai.ac.jp.

doi:10.1158/1078-0432.CCR-09-0478

Translational Relevance

Targeting of IGF-IR is a promising strategy for cancer therapy. CP-751,871 is a fully human monoclonal antibody specific for IGF-IR that inhibits tumor growth in human tumor xenograft models *in vivo*. Although phase II studies of CP-751,871 in combination with chemotherapy are currently underway for certain types of cancer, the effects of CP-751,871 in combination with radiation have not been described. We now show a radiosensitizing effect of CP-751,871 in non–small cell lung cancer cell lines *in vitro* and *in vivo*. Our preclinical data provide a rationale for future clinical investigation of the therapeutic efficacy of CP-751,871 in combination with radiotherapy.

radiotherapy in cancer patients (15). Inhibition of IGF-IR by antisense oligonucleotides, IGF-IR tyrosine kinase inhibitors, or mouse mAbs to the receptor has been shown to enhance the radiosensitivity of tumor cells (16–18). However, the effects of fully human mAbs to IGF-IR on radiosensitivity in cancer cells have not been characterized in detail. We have now examined the effects of the combination of CP-751,871 and radiation on non–small cell lung cancer (NSCLC) cell lines as well as the mechanism responsible for enhancement of radiosensitivity by CP-751,871.

Materials and Methods

Cell culture and reagents. The human NSCLC cell lines National Cancer Institute (NCI)-H292 (H292), NCI-H460 (H460), NCI-H1299 (H1299), LK-2, and NCI-H1975 (H1975) were obtained from American Type Culture Collection (Manassas, VA). The cells were cultured under an atmosphere of 5% CO_2 at 37°C in RPMI 1640 (Sigma, St. Louis, MO) supplemented with 10% fetal bovine serum. Recombinant human IGF-I was obtained from R&D Systems (Minneapolis, MN). CP-751,871 was kindly provided by Pfizer Global Research & Development (Groton, CT).

Immunoblot analysis. Cells were washed twice with ice-cold PBS, and then lysed in a solution containing 20 mmol/L Tris-HCl (pH 7.5), 150 mmol/L NaCl, 1 mmol/L EDTA, 1% Triton X-100, 2.5 mmol/L sodium pyrophosphate, 1 mmol/L phenylmethylsulfonyl fluoride, and leupeptin (1 μg/mL). The protein concentration of lysates was determined with the Bradford reagent (Bio-Rad, Hercules, CA), and equal amounts of protein were subjected to SDS-PAGE on a 7.5% gel. The separated proteins were transferred to a nitrocellulose membrane, which was then exposed to 5% nonfat dried milk in PBS for 1 h at room temperature before incubation overnight at 4°C with rabbit polyclonal antibodies to phosphorylated human IGF-IR (1:1,000 dilution; Cell Signaling, Beverly, MA), to human IGF-IR (1:1,000 dilution; MBL International, Woburn, MA), to phosphorylated human AKT (1:1,000 dilution; Cell Signaling), to human AKT (1:1,000 dilution; Cell Signaling), or to β-actin (1:500 dilution; Sigma). The membrane was then washed with PBS containing 0.05% Tween 20 before incubation for 1 h at room temperature with horseradish peroxidase–conjugated goat antibodies to rabbit IgG (Sigma). Immune complexes were finally detected with chemiluminescence reagents (Perkin-Elmer Life Sciences, Boston, MA).

Flow cytometric analysis of surface IGF-IR expression. Cells (2×10^6) were stained for 2 h at 4°C with an R-phycoerythrin–conjugated mAb to IGF-IR (BD Biosciences, San Jose, CA) or with an isotype-matched control antibody (BD Biosciences). The cells were washed thrice before measurement of fluorescence with a flow cytometer (FACScalibur; Becton Dickinson, San Jose, CA).

Clonogenic survival assay. Exponentially growing cells in 25-cm^2 flasks were harvested by exposure to trypsin and counted. They were diluted serially to appropriate densities, and plated in triplicate in 25-cm^2 flasks containing 10 mL of complete medium in the presence of 50 nmol/L CP-751,871 or vehicle (PBS) before exposure at room temperature to various doses of radiation with a ^{60}Co irradiator at a rate of ~0.82 Gy/min. After incubation for 4 h, the cells were washed with PBS, cultured in antibody-free medium for 10 to 14 d, fixed with methanol/acetic acid (10:1, volume per volume), and stained with crystal violet. Colonies containing >50 cells were counted. The surviving fraction was calculated as: (mean number of colonies)/(number of inoculated cells × plating efficiency). Plating efficiency was defined as the mean number of colonies divided by the number of inoculated cells for the corresponding nonirradiated cells. The surviving fraction for combined treatment was corrected by that for CP-751,871 treatment alone. The dose enhancement factor was then calculated as the dose (Gy) of radiation that yielded a surviving fraction of 0.1 for vehicle-treated cells divided by that for CP-751,871–treated cells (after correction for drug toxicity).

Detection of apoptotic cells. Cells were fixed with 4% paraformaldehyde for 1 h at room temperature, after which a minimum of 1,000 cells per sample was evaluated for apoptosis with the use of the terminal deoxyribonucleotide transferase–mediated nick-end labeling technique (*In situ* Cell Death Detection kit; Boehringer Mannheim, Mannheim, Germany).

Assay of caspase-3 activity. The activity of caspase-3 in cell lysates was measured with a CCP32/Caspase-3 Fluometric Protease Assay kit (MBL). Fluorescence attributable to cleavage of the Asp-Glu-Val-Asp-7-amino-4-trifluoromethyl coumarin (DEVD-AFC) substrate was measured at excitation and emission wavelengths of 390 and 460 nm, respectively.

Immunofluorescence staining of γ-H2AX and Rad51. Cells were grown to 50% confluence in 2-well Lab-Tec Chamber Slides (Nunc, Naperville, IL), deprived of serum overnight, exposed to 10 Gy of radiation in the presence of 50 nmol/L CP-751,871 or vehicle in serum-free medium, incubated for 4 h, and then cultured for various times in complete medium alone. The cells were fixed with 4% paraformaldehyde for 10 min at room temperature, permeabilized with 0.1% Triton X-100 for 10 min at 4°C, and exposed to 5% nonfat dried milk for 10 min at room temperature. They were then washed with PBS and stained overnight at 4°C with mouse mAbs to γ-H2AX (Upstate Biotechnology, Lake Placid, NY) at a dilution of 1:300 and with rabbit polyclonal antibodies to Rad51 (Oncogene Research Products, San Diego, CA) at a dilution of 1:500. Immune complexes were detected by incubation of the slides for 1 h at room temperature with Alexa 488–labeled goat antibodies to mouse IgG (Molecular Probes, Eugene, OR) at a dilution of 1:700 and with Texas red–labeled goat antibodies to rabbit IgG (Vector Laboratories, Burlingame, CA) at a dilution of 1:300. The slides were mounted in fluorescence mounting medium (Dako Cytomation, Hamburg, Germany), and fluorescence signals were visualized with a confocal laser scanning microscope (Axiovert 200M; Carl Zeiss, Oberkochen, Germany) equipped with the LSM 5 PASCAL system (Carl Zeiss). Three random fields, each containing at least 50 cells, were examined at a magnification of ×100, and the percentage of cells containing >5 Rad51 foci per nucleus was determined (19). Nuclei containing ≥10 immunoreactive foci were counted as positive for γ-H2AX, and the percentage of positive cells was calculated (20).

Evaluation of tumor growth in vivo. All animal studies were done in accordance with the Recommendations for Handling of Laboratory Animals for Biomedical Research compiled by the Committee on Safety and Ethical Handling Regulations for Laboratory Animal Experiments, Kyoto University. The ethical procedures followed met the requirements of the United Kingdom Co-ordinating Committee on Cancer Research guidelines (21). Tumor cells (2×10^6) were implanted into the right hind leg of 6-week-old female athymic nude mice (BALB/c *nu/nu*).

Tumor volume was determined from caliper measurement of tumor length (L) and width (W) according to the formula $LW^2/2$. Treatment was initiated when tumors in each group of animals achieved an average volume of ~200 to 250 mm^3. Treatment groups (each containing five mice) consisted of vehicle control (PBS), CP-751,871 alone, vehicle plus radiation, and CP-751,871 plus radiation. CP-751,871 was given i.p. in a single dose of 500 μg per mouse; mice in the control and radiation-alone groups were treated with vehicle (PBS). Mice in the radiation groups received 10 Gy of radiation from a ^{60}Co irradiator either as a single fraction on day 1 of drug treatment or fractionated over 5 consecutive days (days 1 to 5); the radiation was targeted at the tumor, with the remainder of the body shielded with lead. Growth delay (GD) was calculated as the time required to achieve a 5-fold increase in volume for treated tumors minus that for control tumors. The enhancement factor was then determined as:

$$(GD_{combination} - GD_{CP-751,871})/GD_{radiation}.$$

Statistical analysis. Data are presented as means ± SD and were compared between groups with the unpaired Student's *t* test. A *P*-value of <0.05 was considered statistically significant. The effect of the combination of CP-751,871 and radiation on cell survival was assessed by calculation of the combination index with the use of CalcSyn software Biosoft (Cambridge, United Kingdom). Derived from the median-effect principle of Chou and Talalay (22), the combination index provides a quantitative measure of the degree of interaction between ≥2 agents. A combination index of 1 denotes an additive interaction, of >1 denotes antagonism, and of <1 denotes synergy.

Results

IGF-IR expression in NSCLC cells. Immunoblot analysis revealed that IGF-IR was expressed in all human NSCLC cell lines tested (Fig. 1A). Flow cytometry further showed that IGF-IR was expressed at the cell surface in each of these cell lines (Fig. 1B).

CP-751,871 inhibits IGF-IR signaling by blocking IGF-I binding and inducing receptor down-regulation. The efficacy of treatment with mAbs to IGF-IR is thought to be attributable in part to the prevention of ligand binding to the receptor (9). We examined the effects of CP-751,871 on IGF-IR phosphorylation and on activation of the downstream effector AKT induced by ligand stimulation. Immunoblot analysis showed that IGF-I induced marked phosphorylation both of IGF-IR and of the protein kinase AKT in H460 cells, whereas CP-751,871 largely prevented these effects of IGF-I (Fig. 1C). Antibodies to IGF-IR have also been shown to induce receptor down-regulation (12). We also found that CP-751,871 induced a time-dependent decrease in the abundance of IGF-IR in H460 cells, with this effect being pronounced after only 2 hours (Fig. 1D). These results thus suggested that CP-751,871 suppresses IGF-IR signaling through both the direct antagonism of ligand binding and the induction of receptor down-regulation.

CP-751,871 sensitizes NSCLC cells to radiation **in vitro.** To determine whether CP-751,871 affects the sensitivity of NSCLC cells to radiation, we did a clonogenic survival assay. CP-751,871 enhanced the cytotoxic effect of radiation in all tested cell lines (Fig. 2A), with dose enhancement factors of 1.28, 1.20, 1.27, 1.20, and 1.25 for H460, H1299, H292, LK-2, and H1975 cells, respectively. We examined whether the interaction between CP-751,871 and radiation was additive or synergistic by calculating the combination index based on the median-effect principle of Chou and Talalay (22). Synergism with CP-751,871 was apparent at radiation doses of 4, 6, and

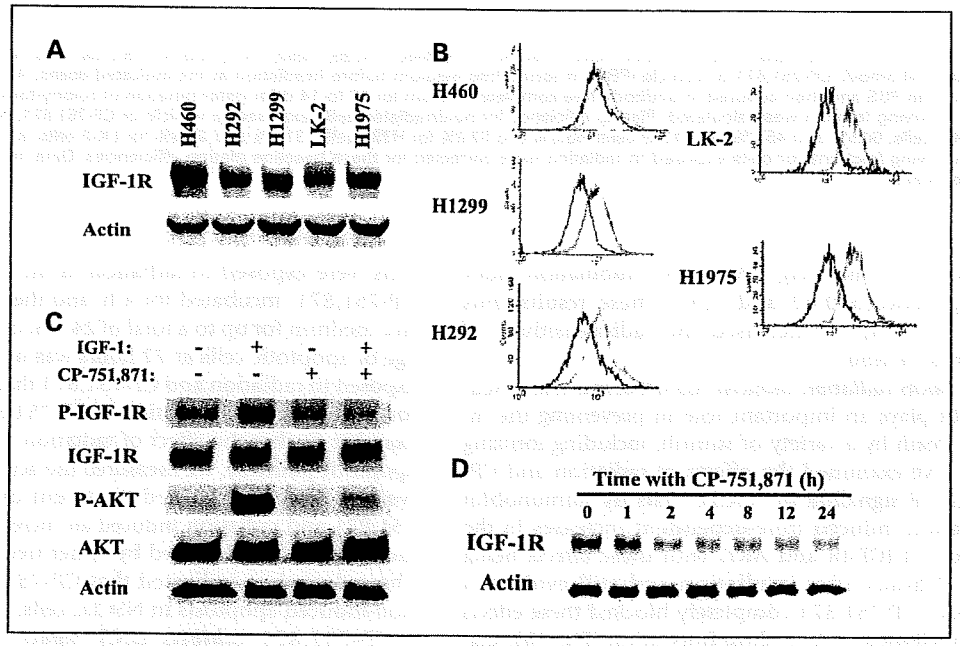

Fig. 1. IGF-1R expression and the effects of CP-751,871 on IGF-IR signaling in human NSCLC cell lines. *A*, H460, H292, H1299, LK-2, and H1975 cells were deprived of serum overnight, lysed, and subjected to immunoblot analysis with antibodies to IGF-IR and to β-actin (loading control). *B*, surface expression of IGF-IR in serum-deprived H460, H1299, H292, LK-2, and H1975 cells was determined by flow cytometry. Representative histograms for cells stained with a mAb to IGF-IR (*green*) or with an isotype-matched control antibody (*black*) are shown. *C*, H460 cells were deprived of serum overnight and then incubated, first in the absence or presence of CP-751,871 (50 nmol/L) for 10 min, and then in the additional absence or presence of IGF-I (50 nmol/L) for 10 min, in serum-free medium. Cell lysates were prepared and subjected to immunoblot analysis with antibodies to phosphorylated (P-) or total forms of IGF-IR or AKT, and to β-actin. *D*, serum-deprived H460 cells were incubated with 50 nmol/L CP-751,871 for the indicated times in serum-free medium, after which cell lysates were subjected to immunoblot analysis with antibodies to IGF-IR and to β-actin.

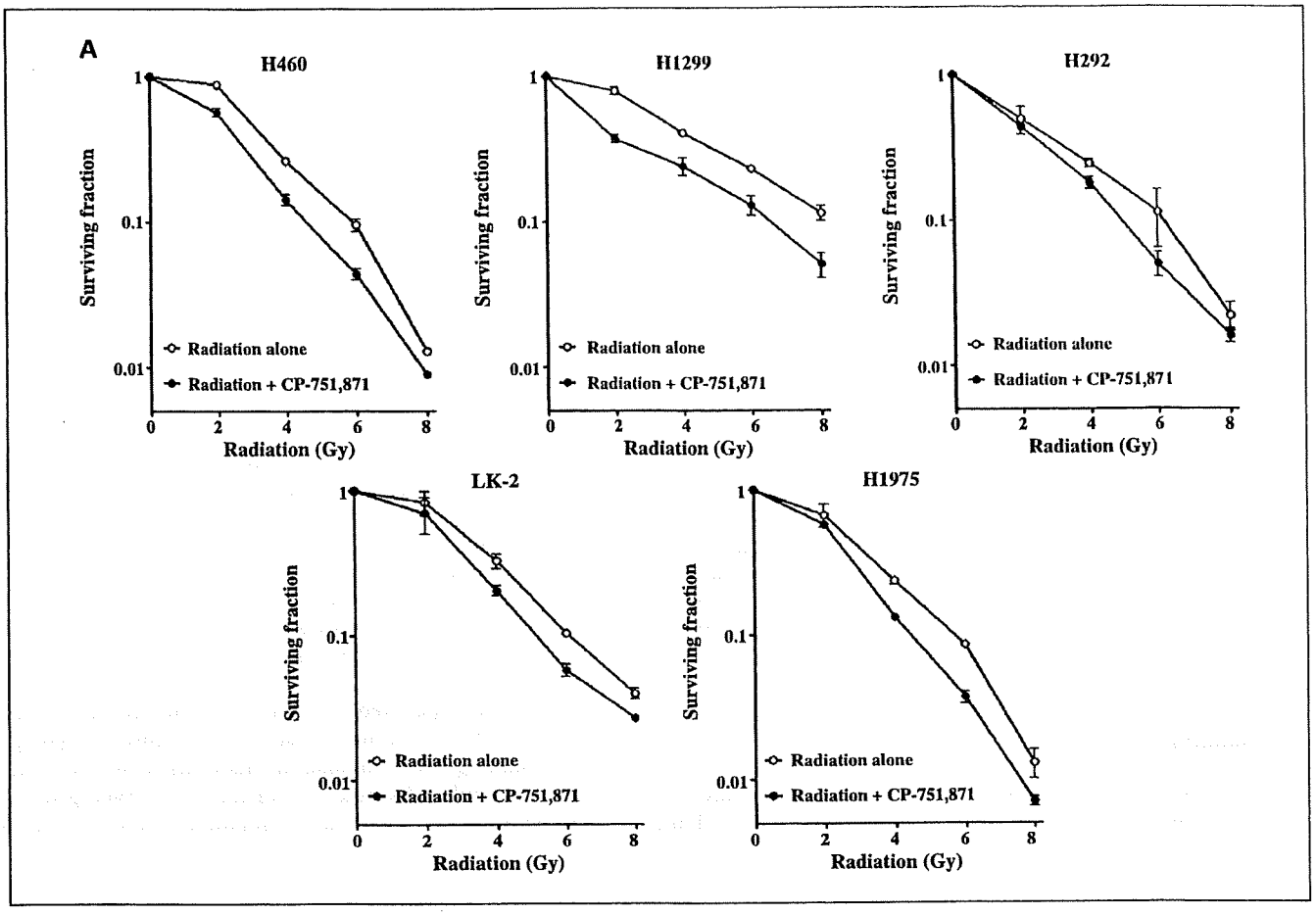

Fig. 2. Effects of CP-751,871 on the sensitivity of NSCLC cells to radiation. *A*, H460, H1299, H292, LK-2, and H1975 cells were deprived of serum overnight, and then exposed to 50 nmol/L CP-751,871 or vehicle (PBS) in serum-free medium before irradiation at the indicated doses. After incubation for 4 h, the cells were washed with PBS and then cultured in antibody-free complete medium for 10 to 14 d for determination of colony-forming ability. Colonies were counted, and the surviving fraction was calculated. Plating efficiency for nonirradiated cells exposed to vehicle or CP-751,871, respectively, was 65.3% and 48.3% for H460 cells, 60.5% and 45.0% for H1299 cells, 63.5% and 52.0% for H292 cells, 31.0% and 27.8% for LK-2 cells, and 87.5% and 52.0% for H1975 cells. All surviving fractions for cells exposed to radiation were corrected for these baseline plating efficiencies. Data, means ± SD from three independent experiments.

8 Gy in all tested cell lines (Fig. 2B), with combination index values ranging between 0.42 and 0.99. These results thus indicated that CP-751,871 increased the radiosensitivity of NSCLC cell lines *in vitro*.

CP-751,871 blocks radiation-induced IGF-IR activation. Activation of IGF-IR plays an important role in preventing the induction of cell death by a variety of stimuli, including ionizing radiation (23). We examined the effects of radiation and CP-751,871 on IGF-IR signaling in NSCLC cells by immunoblot analysis. Radiation induced time-dependent increases in the phosphorylation of IGF-IR and AKT, with these effects being first apparent 2 hours after irradiation and still evident at 8 hours (Fig. 3A). CP-751,871 completely blocked these effects of radiation on IGF-IR and AKT phosphorylation (Fig. 3B), suggesting that radiation-induced activation of IGF-IR in NSCLC cells was inhibited by CP-751,871.

Enhancement of radiation-induced apoptosis by CP-751,871. We next examined whether the inhibitory effect of CP-751,871 on IGF-IR–mediated survival signaling results in enhancement of the proapoptotic activity of radiation. H460 cells were exposed to radiation in the absence or presence of CP-751,871, incubated for 4 h, and then cultured in antibody-free medium for up to a total of 24, 48, or 72 hours. The percentage of apoptotic cells at 72 hours was markedly greater for cells exposed to radiation and CP-751,871 than the sum of the values for cells exposed to radiation or CP-751,871 alone (Fig. 4A). To examine further the effect of radiation and CP-751,871 on the apoptotic pathway, we measured the activity of caspase-3 in cell lysates. Again, combined treatment of H460 cells with CP-751,871 and radiation induced an increase in caspase-3 activity greater than that induced by either treatment alone (Fig. 4B). These data thus indicated that CP-751,871 promoted radiation-induced apoptosis in NSCLC cells.

CP-751,871 inhibits DNA repair in irradiated NSCLC cells. Defects in DNA repair have been associated with enhanced sensitivity of cells to radiation (24), and activated IGF-IR promotes genomic stability by enhancing DNA repair (25). We therefore next investigated the effect of CP-751,871 on DNA repair by immunostaining of cells with antibodies to the phosphorylated form (γ-H2AX) of histone 2AX, foci of which

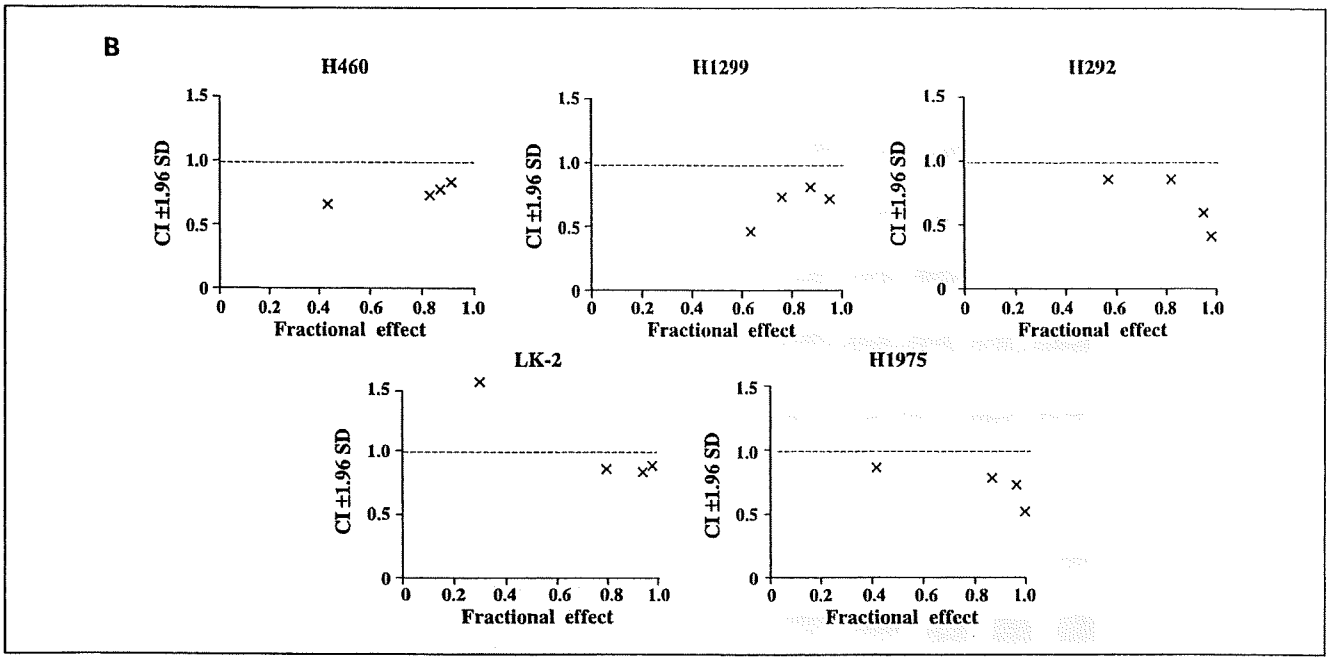

Fig. 2 *Continued. B,* Combination index (CI) plots for CP-751,871 plus radiation. Data represent the algebraic estimate of the CI (±1.96 SD) for 50 nmol/L CP-751,871, and radiation doses of 2, 4, 6, and 8 Gy, and correspond to the results shown in *A.* A CI of 1 denotes an additive interaction, of >1 denotes antagonism, and of <1 denotes synergy.

form at DNA double-strand breaks. Irradiation of H460 cells induced the formation of γ-H2AX foci, with the number of such foci being maximal at ~1 hour and having largely returned to the basal level by 24 hours (Fig. 5A). In the presence of CP-751,871, however, the radiation-induced increase in the number of γ-H2AX foci persisted for at least 24 hours. Evaluation of the percentage of H460 cells with γ-H2AX foci at 24 hours after irradiation revealed that CP-751,871 significantly inhibited the repair of double-strand breaks (Fig. 5B). The formation of γ-H2AX foci has been proposed to result in the recruitment of downstream DNA repair factors to the sites of DNA damage (26). The repair protein Rad51 is a key player in homologous recombination during DNA repair (27). Radiation induced the formation of Rad51 foci in H460 cells, with this effect being maximal at 6 hours and still apparent at 24 hours after irradiation (Fig. 5A and C). The radiation-induced formation of Rad51 foci was largely prevented in the presence of CP-751,871. These results thus suggested that CP-751,871 sensitizes NSCLC cells to radiation by inhibiting the Rad51-dependent repair of radiation-induced double-strand breaks.

CP-751,871 enhances radiation-induced tumor regression. To determine whether the CP-751,871–induced radiosensitization of NSCLC cells observed *in vitro* might also be apparent *in vivo*, we implanted H460 or H1299 cells into nude mice to elicit the formation of solid tumors. After tumor formation, the mice were treated with CP-751,871, radiation, or both modalities. Combined treatment with radiation and CP-751,871 inhibited H460 and H1299 tumor growth to a markedly greater extent than did either modality alone (Fig. 6). The tumor growth delays induced by treatment with radiation alone, CP-751,871 alone, or both CP-751,871 and radiation were 13.3, 5.4, and 23.7 days, respectively, for H460 cells; and 1.6, 1.6, and 8.6 days, respectively, for H1299 cells. The enhancement factor for the effect of CP-751,871 on the efficacy of radiation was 1.4 for H460 cells and 4.4 for H1299 cells, revealing the effect to be greater than additive. No pronounced tissue damage or toxicity, such as weight loss, was observed in mice in any of the treatment groups.

Finally, we evaluated whether the combination of CP-751,871 and fractionated radiation treatment would result in inhibition of tumor growth similar to that observed with CP-751,871 plus single-fraction radiation. We examined only the H460 xenograft model in the fractionated radiotherapy experiments. The tumor growth delays induced by treatment with radiation alone, CP-751,871 alone, or both CP-751,871 and radiation were 6.4, 2.7, and 27.2 days, respectively (Supplementary Fig. S1). The enhancement factor for the effect of CP-751,871 on the efficacy of radiation was 3.8. Again, there was no evidence of toxicity, such as body weight loss, and there were no animal deaths in any of the four groups. These data suggested that CP-751,871 enhances the tumor response to both single-dose and fractionated radiotherapy *in vivo*.

Discussion

Several mAbs to IGF-IR that block ligand binding and induce receptor down-regulation have been developed (8, 9). We have now shown that CP-751,871 suppresses IGF-IR signaling through direct antagonism of ligand binding and receptor down-regulation. We also found that CP-751,871 sensitizes tumor cells to radiation *in vitro*, and that combination treatment with CP-751,871 and radiation results in a greater-than-additive delay in tumor growth in tumor xenograft models without systemic toxicity. The mechanism by which CP-751,871 enhances radiosensitivity seems to involve inhibition of the repair

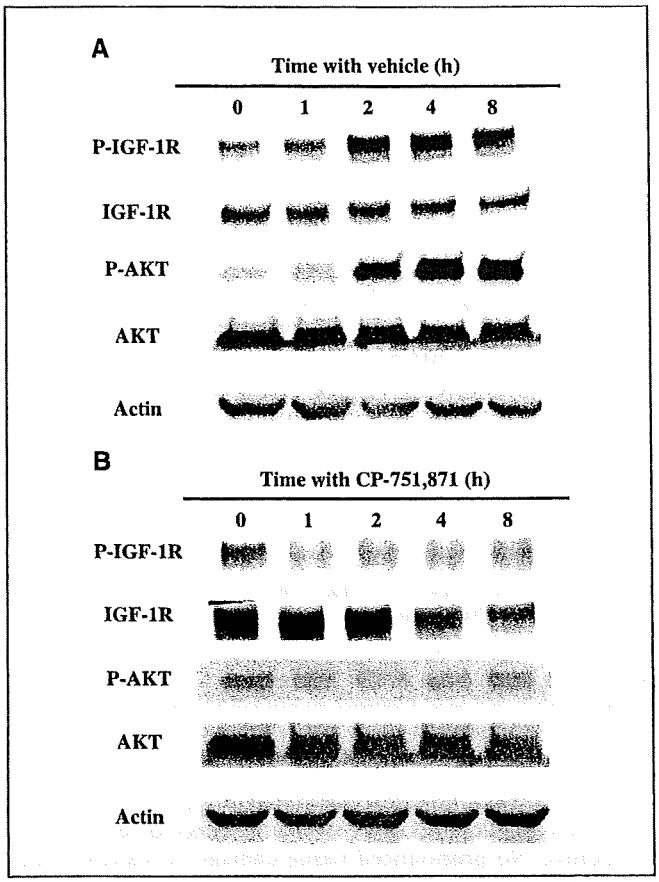

Fig. 3. Effects of CP-751,871 on IGF-IR and AKT phosphorylation induced by radiation. Serum-deprived H460 cells were exposed to 10 Gy of radiation in the absence (*A*) or presence (*B*) of 50 nmol/L CP-751,871 in serum-free medium. Cell lysates were prepared at the indicated times after irradiation and subjected to immunoblot analysis with antibodies to phosphorylated or total forms of IGF-IR or AKT, and to β-actin.

of radiation-induced double-strand breaks and potentiation of cancer cell apoptosis.

Cellular stress induced by several chemotherapeutic agents or radiation triggers the activation of IGF-IR signaling (14, 28, 29). We found that radiation induced IGF-IR phosphorylation in NSCLC cells. Other growth factor receptors, such as the epidermal growth factor receptor, are also activated by radiation (30, 31). Reactive oxygen species and reactive nitrogen species generated by radiation are thought to shift the steady-state tyrosine phosphorylation status of epidermal growth factor receptor to the phosphorylated (active) form as a result of the inactivation of critical cysteine residues in the catalytic center of corresponding protein phosphatases (32–34). Activated epidermal growth factor receptor signaling in turn promotes the release of paracrine ligands, such as the pro form of transforming growth factor α, and the consequent activation of receptors and intracellular signaling pathways (35). The insulin receptor is a receptor tyrosine kinase that is also activated by a reactive oxygen species–dependent mechanism (30, 36). Although the precise mechanism by which radiation induces IGF-IR phosphorylation remains to be elucidated, these previous observations suggest that radiation-induced IGF-IR activation may occur in ligand-dependent or ligand-independent manners. We found that CP-751,871 blocked radiation-induced IGF-IR activation, likely as a result of both competition with ligand for binding to IGF-IR and receptor down-regulation. Given that radiation-induced IGF-IR phosphorylation contributes to radiation-induced acceleration of tumor cell repopulation and enhancement of radioresistance (37), our data indicate that CP-751,871 increases radiosensitivity by suppressing radiation-induced IGF-IR activation.

IGF-IR activation results in suppression of apoptosis signaling pathways and promotion of cell survival. Previous studies have shown that another type of antibody to IGF-IR promotes apoptotic cell death (8, 38). In the present study, we found that the combination of CP-751,871 and radiation induced NSCLC cell apoptosis as well as the activation of caspase-3 to an extent greater than that apparent with either agent alone. Our data thus suggest that CP-751,871 inhibits antiapoptotic signaling elicited by radiation-induced IGF-IR activation. However, the fraction of apoptotic cells detected under our experimental conditions was relatively small. Given that the relation between apoptosis and radiosensitivity is controversial (39–41), we examined additional mechanisms by which CP-751,871 might contribute to radiosensitization.

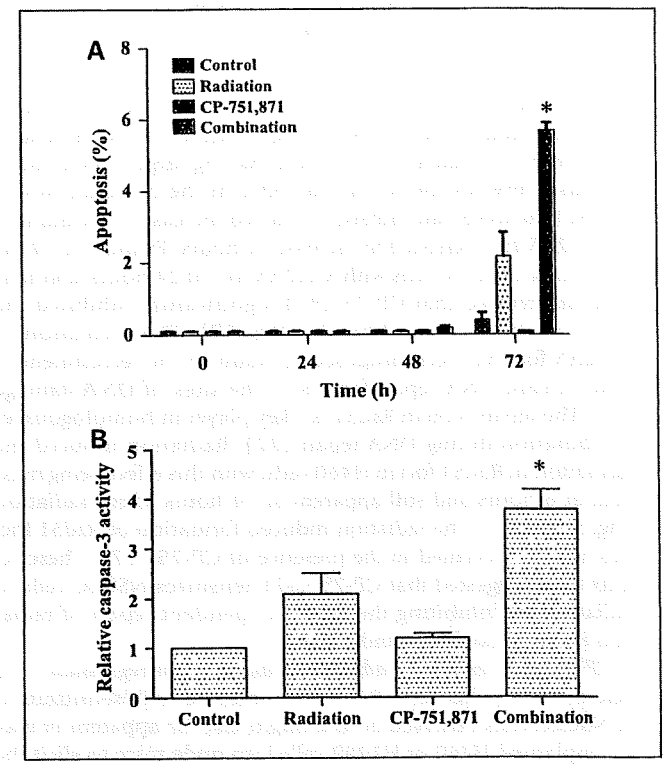

Fig. 4. Effects of CP-751,871 on radiation-induced apoptosis and caspase-3 activity in H460 cells. *A*, serum-deprived H460 cells were exposed (or not) to 10 Gy of radiation in the presence of 50 nmol/L CP-751,871 or vehicle (PBS) in serum-free medium, incubated for 4 h, and then cultured in antibody-free complete medium for up to a total of 24, 48, or 72 h. The percentage of apoptotic cells was then determined by terminal deoxyribonucleotide transferase–mediated nick-end labeling staining. *B*, lysates of cells treated as in *A* were assayed for caspase-3 activity 72 h after irradiation. Data, means ± SD from three independent experiments; those in *B* are expressed relative to the corresponding value for the control condition. *, $P < 0.01$ versus the corresponding value for treatment with radiation or CP-751,871 alone.

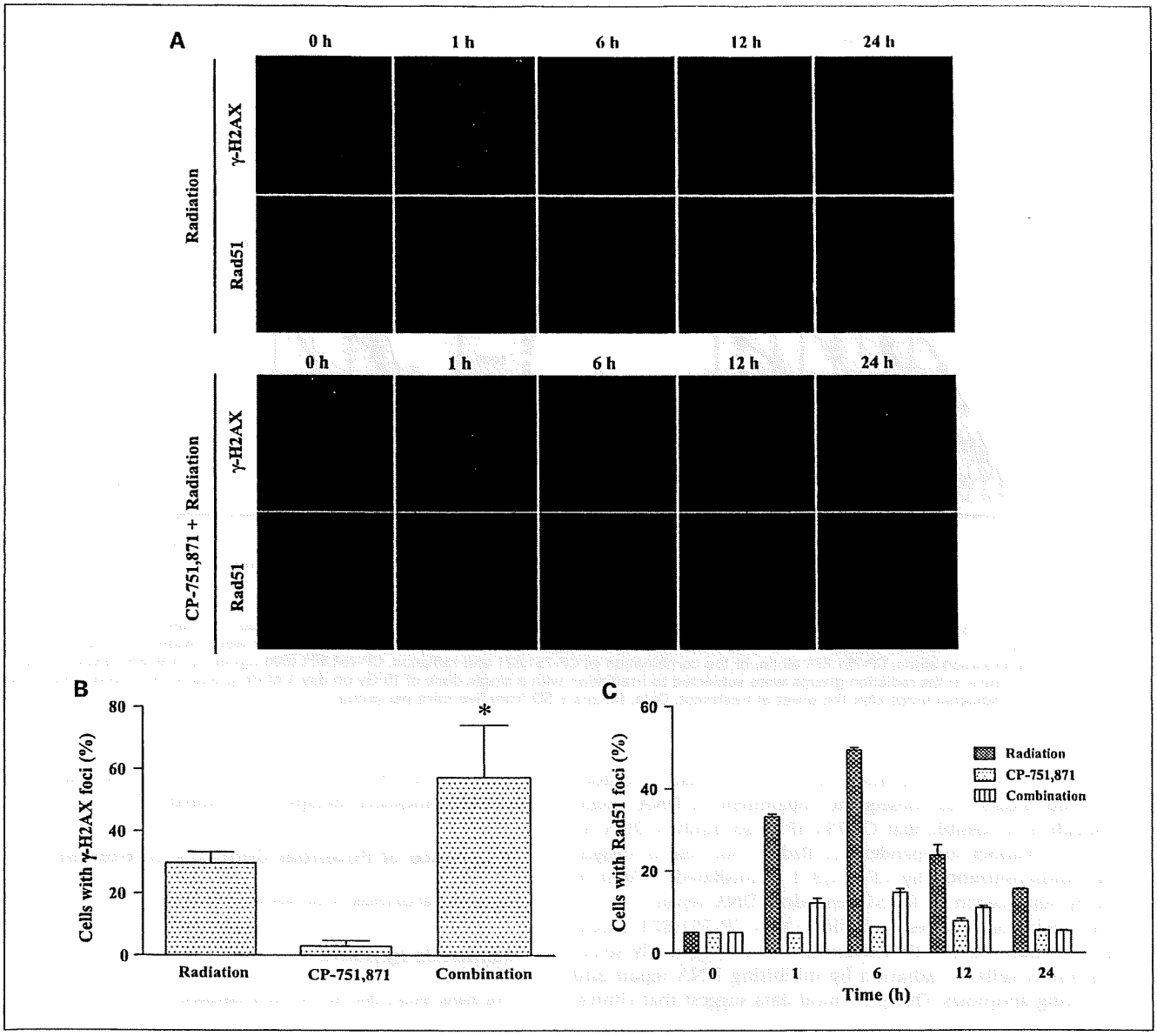

Fig. 5. Effects of CP-751,871 on the radiation-induced formation of γ-H2AX and Rad51 foci in H460 cells. *A*, serum-deprived cells were exposed to 10 Gy of radiation in the presence of vehicle (PBS) or 50 nmol/L CP-751,871 in serum-free-medium, incubated for 4 h, and then cultured for up to the indicated total times in antibody-free complete medium. The cells were then fixed and subjected to immunofluorescence staining for γ-H2AX (*green fluorescence*) and Rad51 (*red fluorescence*). *B*, cells treated as in *A* were fixed at 24 h after irradiation, and the percentage of cells containing γ-H2AX foci was determined. Data, means ± SD from three independent experiments. *, $P < 0.05$ versus the corresponding value for cells exposed to radiation or CP-751,871 alone. *C*, cells treated as in *A* were evaluated for the percentage of cells containing Rad51 foci. Data, means ± SD from three independent experiments.

The IGF-IR signaling pathway has been implicated in regulation of DNA repair (29, 42, 43). We investigated the effects of CP-751,871 on the repair of radiation-induced DNA damage by immunofluorescence staining of γ-H2AX. Given that γ-H2AX appears rapidly at DNA double-strand breaks and disappears as repair proceeds (44), it serves as a sensitive and specific marker for unrepaired DNA damage. We found that CP-751,871 inhibited the repair of radiation-induced double-strand breaks. Ligand-induced IGF-IR activation was previously shown to attenuate a cytosolic interaction between the DNA repair protein Rad51 and insulin receptor substrate 1, a key mediator of IGF-IR signaling, resulting in the translocation of Rad51 to the sites of DNA double-strand breaks (43). Given that radiation induced IGF-IR activation, we examined whether CP-751,871 in combination with radiation might affect the subcellular distribution of Rad51. We found that radiation increased the number of nuclear Rad51 foci, likely as a result of radiation-induced IGF-IR activation, whereas CP-751,871 inhibited this effect. These results indicate that prevention of radiation-induced IGF-IR activation by

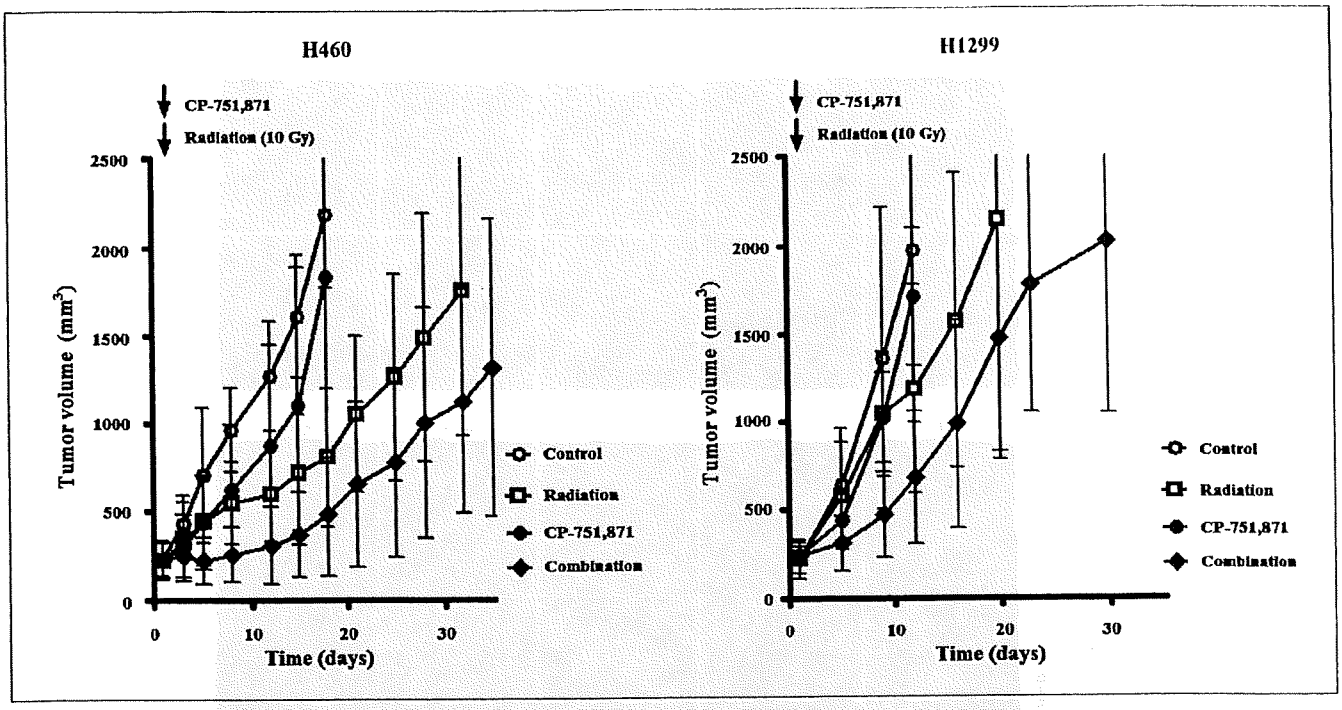

Fig. 6. Effects of CP-751,871 on the growth of H460 or H1299 tumors in mice subjected to single-dose radiotherapy. H460 or H1299 cells were implanted into the right hind limb of nude mice and allowed to form tumors with an average volume of ~200 to 250 mm^3. The mice were divided into four treatment groups: control, radiation alone, CP-751,871 alone, or the combination of CP-751,871 and radiation. CP-751,871 (500 μg) or vehicle was given i.p. in a single dose, and mice in the radiation groups were subjected to irradiation with a single dose of 10 Gy on day 1 of drug treatment. Tumor volume was measured at the indicated times after the onset of treatment. Data, means ± SD from five mice per group.

CP-751,871 results in insufficient recruitment of Rad51 to double-strand breaks and consequent impairment of DNA repair. Although it is possible that CP-751,871 also inhibits DNA repair in a manner independent of Rad51, our results suggest that radiosensitization by CP-751,871 is mediated at least in part by suppression of Rad51-dependent DNA repair.

In conclusion, our results indicate that CP-751,871 blocks radiation-induced IGF-IR activation, and consequently sensitizes tumor cells to radiation by inhibiting DNA repair and promoting apoptosis. Our preclinical data suggest that clinical evaluation of CP-751,871 in combination with radiation as a potential anticancer therapy is warranted.

Disclosure of Potential Conflicts of Interest

No potential conflicts of interest were disclosed.

Acknowledgments

We thank Shoko Ono for technical assistance.

References

1. Sell C, Rubini M, Rubin R, Liu JP, Efstratiadis A, Baserga R. Simian virus 40 large tumor antigen is unable to transform mouse embryonic fibroblasts lacking type 1 insulin-like growth factor receptor. Proc Natl Acad Sci U S A 1993;90:11217–21.
2. O'Connor R, Kauffmann-Zeh A, Liu Y, et al. Identification of domains of the insulin-like growth factor I receptor that are required for protection from apoptosis. Mol Cell Biol 1997;17:427–35.
3. Pietrzkowski Z, Mulholland G, Gomella L, Jameson BA, Wernicke D, Baserga R. Inhibition of growth of prostatic cancer cell lines by peptide analogues of insulin-like growth factor 1. Cancer Res 1993;53:1102–6.
4. D'Ambrosio C, Ferber A, Resnicoff M, Baserga R. A soluble insulin-like growth factor I receptor that induces apoptosis of tumor cells *in vivo* and inhibits tumorigenesis. Cancer Res 1996;56:4013–20.
5. Muller M, Dietel M, Turzynski A, Wiechen K. Antisense phosphorothioate oligodeoxynucleotide down-regulation of the insulin-like growth factor I receptor in ovarian cancer cells. Int J Cancer 1998;77:567–71.
6. Scotlandi K, Avnet S, Benini S, et al. Expression of an IGF-I receptor dominant negative mutant induces apoptosis, inhibits tumorigenesis and enhances chemosensitivity in Ewing's sarcoma cells. Int J Cancer 2002;101:11–6.
7. Garcia-Echeverria C, Pearson MA, Marti A, et al. *In vivo* antitumor activity of NVP-AEW541-a novel, potent, and selective inhibitor of the IGF-IR kinase. Cancer Cell 2004;5:231–9.
8. Maloney EK, McLaughlin JL, Dagdigian NE, et al. An anti-insulin-like growth factor I receptor antibody that is a potent inhibitor of cancer cell proliferation. Cancer Res 2003;63:5073–83.
9. Burtrum D, Zhu Z, Lu D, et al. A fully human monoclonal antibody to the insulin-like growth factor I receptor blocks ligand-dependent signaling and inhibits human tumor growth *in vivo*. Cancer Res 2003;63:8912–21.
10. Cohen BD, Baker DA, Soderstrom C, et al. Combination therapy enhances the inhibition of tumor growth with the fully human anti-type 1 insulin-like growth factor receptor monoclonal antibody CP-751,871. Clin Cancer Res 2005;11:2063–73.
11. Wang Y, Hailey J, Williams D, et al. Inhibition of insulin-like growth factor-I receptor (IGF-IR) signaling and tumor cell growth by a fully human neutralizing anti-IGF-IR antibody. Mol Cancer Ther 2005;4:1214–21.
12. Sachdev D, Yee D. Disrupting insulin-like growth factor signaling as a potential cancer therapy. Mol Cancer Ther 2007;6:1–12.
13. Garber K. IGF-1: old growth factor shines as new drug target. J Natl Cancer Inst 2005;97:790–2.
14. Turner BC, Haffty BG, Narayanan L, et al.

Insulin-like growth factor-I receptor overexpression mediates cellular radioresistance and local breast cancer recurrence after lumpectomy and radiation. Cancer Res 1997;57:3079–83.
15. Rocha RL, Hilsenbeck SG, Jackson JG, et al. Insulin-like growth factor binding protein-3 and insulin receptor substrate-1 in breast cancer: correlation with clinical parameters and disease-free survival. Clin Cancer Res 1997;3:103–9.
16. Kuhn C, Hurwitz SA, Kumar MG, Cotton J, Spandau DF. Activation of the insulin-like growth factor-1 receptor promotes the survival of human keratinocytes following ultraviolet B irradiation. Int J Cancer 1999;80:431–8.
17. Wen B, Deutsch E, Marangoni E, et al. Tyrphostin AG 1024 modulates radiosensitivity in human breast cancer cells. Br J Cancer 2001; 85:2017–21.
18. Cosaceanu D, Carapancea M, Castro J, et al. Modulation of response to radiation of human lung cancer cells following insulin-like growth factor 1 receptor inactivation. Cancer Lett 2005;222:173–81.
19. Sak A, Stueben G, Groneberg M, Bocker W, Stuschke M. Targeting of Rad51-dependent homologous recombination: implications for the radiation sensitivity of human lung cancer cell lines. Br J Cancer 2005;92:1089–97.
20. Albert JM, Cao C, Kim KW, et al. Inhibition of poly(ADP-ribose) polymerase enhances cell death and improves tumor growth delay in irradiated lung cancer models. Clin Cancer Res 2007;13:3033–42.
21. United Kingdom Co-ordinating Committee on Cancer Research. Guidelines for the welfare of animals in experimental neoplasia (2nd ed.). Br J Cancer 1998;77:1–10.
22. Chou TC, Talalay P. Quantitative analysis of dose-effect relationships: the combined effects of multiple drugs or enzyme inhibitors. Adv Enzyme Regul 1984;22:27–55.
23. Tezuka M, Watanabe H, Nakamura S, et al. Antiapoptotic activity is dispensable for insulin-like growth factor I receptor-mediated clonogenic radioresistance after γ-irradiation. Clin Cancer Res 2001;7:3206–14.
24. Gao Y, Ferguson DO, Xie W, et al. Interplay of p53 and DNA-repair protein XRCC4 in tumorigenesis, genomic stability and development. Nature 2000;404:897–900.
25. Yang S, Chintapalli J, Sodagum L, et al. Activated IGF-1R inhibits hyperglycemia-induced DNA damage and promotes DNA repair by homologous recombination. Am J Physiol Renal Physiol 2005;289:F1144–52.
26. Burma S, Chen BP, Murphy M, Kurimasa A, Chen DJ. ATM phosphorylates histone H2AX in response to DNA double-strand breaks. J Biol Chem 2001;276:42462–7.
27. Chen G, Yuan SS, Liu W, et al. Radiation-induced assembly of Rad51 and Rad52 recombination complex requires ATM and c-Abl. J Biol Chem 1999;274:12748–52.
28. Gooch JL, Van Den Berg CL, Yee D. Insulin-like growth factor (IGF)-I rescues breast cancer cells from chemotherapy-induced cell death-proliferative and anti-apoptotic effects. Breast Cancer Res Treat 1999;56:1–10.
29. Cosaceanu D, Budiu RA, Carapancea M, Castro J, Lewensohn R, Dricu A. Ionizing radiation activates IGF-1R triggering a cytoprotective signaling by interfering with Ku-DNA binding and by modulating Ku86 expression via a p38 kinase-dependent mechanism. Oncogene 2007;26:2423–34.
30. Bowers G, Reardon D, Hewitt T, et al. The relative role of ErbB1-4 receptor tyrosine kinases in radiation signal transduction responses of human carcinoma cells. Oncogene 2001;20:1388–97.
31. Griffin RJ, Williams BW, Wild R, Cherrington JM, Park H, Song CW. Simultaneous inhibition of the receptor kinase activity of vascular endothelial, fibroblast, and platelet-derived growth factors suppresses tumor growth and enhances tumor radiation response. Cancer Res 2002;62:1702–6.
32. Schmidt-Ullrich RK, Dent P, Grant S, Mikkelsen RB, Valerie K. Signal transduction and cellular radiation responses. Radiat Res 2000;153: 245–57.
33. Leach JK, Van Tuyle G, Lin PS, Schmidt-Ullrich R, Mikkelsen RB. Ionizing radiation-induced, mitochondria-dependent generation of reactive oxygen/nitrogen. Cancer Res 2001;61: 3894–901.
34. Leach JK, Black SM, Schmidt-Ullrich RK, Mikkelsen RB. Activation of constitutive nitric-oxide synthase activity is an early signaling event induced by ionizing radiation. J Biol Chem 2002;277:15400–6.
35. Shvartsman SY, Hagan MP, Yacoub A, Dent P, Wiley HS, Lauffenburger DA. Autocrine loops with positive feedback enable context-dependent cell signaling. Am J Physiol Cell Physiol 2002;282: C545–59.
36. Dent P, Han SI, Mitchell C, et al. Inhibition of insulin/IGF-1 receptor signaling enhances bile acid toxicity in primary hepatocytes. Biochem Pharmacol 2005;70:1685–96.
37. Dent P, Yacoub A, Contessa J, et al. Stress and radiation-induced activation of multiple intracellular signaling pathways. Radiat Res 2003;159: 283–300.
38. Benini S, Manara MC, Baldini N, et al. Inhibition of insulin-like growth factor I receptor increases the antitumor activity of doxorubicin and vincristine against Ewing's sarcoma cells. Clin Cancer Res 2001;7:1790–7.
39. Akagi Y, Ito K, Sawada S. Radiation-induced apoptosis and necrosis in Molt-4 cells: a study of dose-effect relationships and their modification. Int J Radiat Biol 1993;64: 47–56.
40. Lawrence TS, Davis MA, Hough A, Rehemtulla A. The role of apoptosis in 2',2'-difluoro-2'-deoxycytidine (gemcitabine)-mediated radiosensitization. Clin Cancer Res 2001;7:314–9.
41. Pawlik TM, Keyomarsi K. Role of cell cycle in mediating sensitivity to radiotherapy. Int J Radiat Oncol Biol Phys 2004;59:928–42.
42. Heron-Milhavet L, LeRoith D. Insulin-like growth factor I induces MDM2-dependent degradation of p53 via the p38 MAPK pathway in response to DNA damage. J Biol Chem 2002;277: 15600–6.
43. Trojanek J, Ho T, Del Valle L, et al. Role of the insulin-like growth factor I/insulin receptor substrate 1 axis in Rad51 trafficking and DNA repair by homologous recombination. Mol Cell Biol 2003;23:7510–24.
44. Rogakou EP, Pilch DR, Orr AH, Ivanova VS, Bonner WM. DNA double-stranded breaks induce histone H2AX phosphorylation on serine 139. J Biol Chem 1998;273:5858–68.

Sorafenib Inhibits Non–Small Cell Lung Cancer Cell Growth by Targeting B-RAF in *KRAS* Wild-Type Cells and C-RAF in *KRAS* Mutant Cells

Ken Takezawa,[1] Isamu Okamoto,[1] Kimio Yonesaka,[1] Erina Hatashita,[1] Yuki Yamada,[1] Masahiro Fukuoka,[2] and Kazuhiko Nakagawa[1]

[1]Department of Medical Oncology, Kinki University School of Medicine; [2]Department of Medical Oncology, Kinki University School of Medicine, Sakai Hospital, Osaka, Japan

Abstract

Sorafenib is a multikinase inhibitor whose targets include B-RAF and C-RAF, both of which function in the extracellular signal-regulated kinase (ERK) signaling pathway but which also have distinct downstream targets. The relative effects of sorafenib on B-RAF and C-RAF signaling in tumor cells remain unclear, however. We have now examined the effects of sorafenib as well as of B-RAF or C-RAF depletion by RNA interference on cell growth and ERK signaling in non–small cell lung cancer (NSCLC) cell lines with or without *KRAS* mutations. Sorafenib inhibited ERK phosphorylation in cells with wild-type *KRAS* but not in those with mutant *KRAS*. Despite this difference, sorafenib inhibited cell growth and induced G_1 arrest in both cell types. Depletion of B-RAF, but not that of C-RAF, inhibited ERK phosphorylation as well as suppressed cell growth and induced G_1 arrest in cells with wild-type *KRAS*. In contrast, depletion of C-RAF inhibited cell growth and induced G_1 arrest, without affecting ERK phosphorylation, in cells with mutant *KRAS*; depletion of B-RAF did not induce G_1 arrest in these cells. These data suggest that B-RAF-ERK signaling and C-RAF signaling play the dominant roles in regulation of cell growth in NSCLC cells with wild-type or mutant *KRAS*, respectively. The G_1 arrest induced by either C-RAF depletion or sorafenib in cells with mutant *KRAS* was associated with down-regulation of cyclin E. Our results thus suggest that sorafenib inhibits NSCLC cell growth by targeting B-RAF in cells with wild-type *KRAS* and C-RAF in those with mutant *KRAS*. [Cancer Res 2009;69(16):6515–21]

Introduction

Lung cancer is the leading cause of cancer-related mortality worldwide (1). Treatment options are limited for patients with advanced metastatic lung cancer, with traditional cytotoxic chemotherapy conferring only a limited survival benefit. Target-based therapies are therefore being pursued as potential treatment alternatives. The RAS-RAF-mitogen-activated protein kinase (MAPK)/extracellular signal-regulated kinase (ERK) kinase-ERK signaling pathway is a promising therapeutic target given its central role in regulation of mammalian cell proliferation, relaying extracellular signals from ligand-bound receptor tyrosine kinases (RTK) at the cell surface to the nucleus via a cascade of specific phosphorylation events and beginning with the activation of the small GTPase RAS (2). Much attention is thus being focused on the development of inhibitors of this pathway.

RAF was the first effector kinase downstream of RAS to be identified (3). To date, the most successful clinical inhibitor of RAF activity is sorafenib (Nexavar, BAY 43-9006), an orally available compound that has received approval by the U.S. Food and Drug Administration for the treatment of advanced renal cell carcinoma and hepatocellular carcinoma. Sorafenib is also currently undergoing clinical evaluation for a variety of additional cancers, including non–small cell lung cancer (NSCLC; refs. 4–7).

The mutational status of *RAS* and *B-RAF* genes is thought to affect the sensitivity of tumor cell lines to sorafenib as a result of the inappropriate activation by such mutations of the MAPK pathway mediated by ERK (8, 9). The sensitivity of tumor cell lines with different *RAS* mutations to sorafenib is less well characterized than is that of those with *B-RAF* mutations (10–14). Despite promising results of clinical trials of sorafenib monotherapy in NSCLC patients (4–7), little is known of the possible differences in the sorafenib sensitivity of NSCLC cells according to the mutational status of *KRAS*. We have therefore now examined the effects of RAF inhibition on the growth of NSCLC cells with or without *KRAS* mutations and further investigated the mechanisms of such effects.

Materials and Methods

Cell culture and reagents. The human NSCLC cell lines NCI-H292 (H292), LK-2, Sq-1, NCI-H520 (H520), PC9, NCI-H1650 (H1650), HCC827, NCI-H1975 (H1975), A549, NCI-H460 (H460), NCI-H23 (H23), NCI-H358 (H358), and NCI-H1299 (H1299) were obtained from the American Type Culture Collection. Ma70 cells were obtained as previously described (15). All cells were cultured under a humidified atmosphere of 5% CO_2 at 37°C in RPMI 1640 (Sigma) supplemented with 10% fetal bovine serum. Sorafenib was kindly provided by Bayer Pharmaceutical, dissolved in DMSO, and stored in aliquots at −20°C.

Assay of anchorage-dependent cell growth [3-(4,5-dimethylthiazol-2-yl)-2,5-diphenyltetrazolium bromide assay]. Cells were plated in 96-well flat-bottomed plates and cultured for 24 h before exposure to various concentrations of sorafenib for 72 h. TetraColor One (5 mmol/L tetrazolium monosodium salt and 0.2 mmol/L 1-methoxy-5-methyl phenazinium methylsulfate; Seikagaku) was then added to each well, and the cells were incubated for 3 h at 37°C before measurement of absorbance at 490 nm with a Multiskan Spectrum instrument (Thermo Labsystems). Absorbance values were expressed as a percentage of that for untreated cells, and the concentration of sorafenib resulting in 50% growth inhibition (IC_{50}) was calculated.

Assay of anchorage-independent colony formation in soft agar. Anchorage-independent cell proliferation in soft agar was assayed with the use of a CytoSelect 96-Well Cell Transformation Assay (Cell Biolabs). In brief, cells were cultured for 7 d in complete medium containing soft agar and various concentrations of sorafenib. The agar matrix was then solubilized, the cells were stained with 3-(4,5-dimethylthiazol-2-yl)-2,5-diphenyltetrazolium

Requests for reprints: Isamu Okamoto, Department of Medical Oncology, Kinki University School of Medicine, 377-2 Ohno-higashi, Osaka-Sayama, Osaka 589-8511, Japan. Phone: 81-72-366-0221; Fax: 81-72-360-5000; E-mail: chi-okamoto@dotd.med.kindai.ac.jp.

doi:10.1158/0008-5472.CAN-09-1076

bromide (MTT) and lysed, and the absorbance at 570 nm was measured relative to that at a reference wavelength of 690 nm. Normalized absorbance values were expressed as a percentage of that for untreated cells, and the IC_{50} of sorafenib for inhibition of colony formation was calculated.

Cell cycle analysis. Cells were harvested, washed with PBS, fixed with 70% methanol, washed again with PBS, and stained with propidium iodide (0.05 mg/mL) in a solution containing 0.1% Triton X-100, 0.1 mmol/L EDTA, and RNase A (0.05 mg/mL). The stained cells ($\sim 1 \times 10^6$) were then analyzed for DNA content with a flow cytometer (FACSCalibur, Becton Dickinson) and ModFit software (Verity Software House).

Immunoblot analysis. Cells were washed twice with ice-cold PBS and then lysed in a solution containing 20 mmol/L Tris-HCl (pH 7.5), 150 mmol/L NaCl, 1 mmol/L EDTA, 1% Triton X-100, 2.5 mmol/L sodium pyrophosphate, 1 mmol/L phenylmethylsulfonyl fluoride, and 1 μg/mL leupeptin. The protein concentration of lysates was determined with the Bradford reagent (Bio-Rad), and equal amounts of protein were subjected to SDS-PAGE on a 7.5% gel. The separated proteins were transferred to a nitrocellulose membrane, which was then exposed to 5% nonfat dried milk in PBS for 1 h at room temperature before incubation overnight at 4°C with rabbit polyclonal antibodies to human phosphorylated ERK (1:1,000 dilution; Santa Cruz Biotechnology), ERK (1:1,000 dilution; Santa Cruz Biotechnology), FLAG epitope (1:1,000 dilution; Cell Signaling Technology), B-RAF (1:1,000 dilution; Santa Cruz Biotechnology), C-RAF (1:1,000 dilution; Cell Signaling Technology), or β-actin (1:500 dilution; Sigma) or with mouse monoclonal antibodies to cyclin E (1:1,000 dilution; Santa Cruz Biotechnology). The membrane was then washed with PBS containing 0.05% Tween 20 before incubation for 1 h at room temperature with horseradish peroxidase–conjugated goat antibodies to rabbit (Sigma) or mouse (Santa Cruz Biotechnology) immunoglobulin G. Immune complexes were finally detected with chemiluminescence reagents (Perkin-Elmer Life Science).

Forced expression of KRAS-V12. An expression vector for FLAG-tagged human KRAS-V12 was constructed by inserting the corresponding cDNA into the pcDNA3 plasmid (Invitrogen). The expression vector was introduced into H1299 cells by transfection for 48 h with the use of the Lipofectamine 2000 reagent (Invitrogen).

Gene silencing. Cells were plated at 50% to 60% confluence in six-well plates or 25-cm^2 flasks and then incubated for 24 h before transient transfection for 48 h with small interfering RNAs (siRNAs) mixed with the Lipofectamine reagent. The siRNAs specific for B-RAF (5′-AGACAGGAAUCGAAUGAAA-3′) or C-RAF (5′-CCUCACGCCUUCACCUUUA-3′) mRNAs were obtained from Dharmacon, and a nonspecific siRNA (control) was obtained from Nippon EGT. The cells were then subjected to immunoblot analysis or flow cytometry.

Statistical analysis. Data were analyzed by Student's two-tailed *t* test. A *P* value of <0.05 was considered statistically significant.

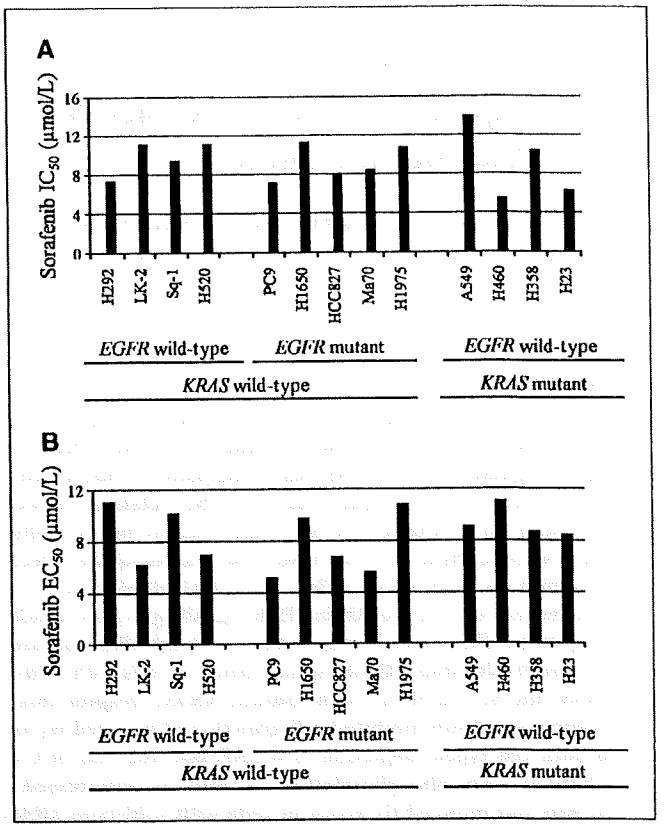

Figure 1. Effects of sorafenib on the growth of NSCLC cell lines classified according to *KRAS* and *EGFR* mutational status. *A*, the indicated NSCLC cell lines were cultured for 72 h in complete culture medium containing various concentrations of sorafenib, after which cell viability was assessed with the MTT assay and the IC_{50} values of sorafenib for inhibition of cell growth were determined. *B*, the indicated NSCLC cell lines were cultured for 7 d in complete medium containing soft agar and various concentrations of sorafenib, after which colony formation was evaluated and the IC_{50} values of sorafenib for inhibition of anchorage-independent cell proliferation were determined. All data are means of triplicates from representative experiments that were repeated on three separate occasions.

Results

Sorafenib inhibits cell growth by inducing G_1 arrest in NSCLC cell lines independently of *KRAS* genotype. The various isoforms of RAF are the principal effectors of RAS in the ERK signaling pathway, and mutant RAS proteins trigger persistent activation of downstream effectors (3). To determine whether the mutational status of *KRAS* might affect the sensitivity of NSCLC cells to sorafenib, an inhibitor of the kinase activity of RAF (16), we first examined the effects of this drug on the anchorage-dependent growth of NSCLC cells with or without *KRAS* mutations by the MTT assay. Sorafenib inhibited cell growth with IC_{50} values ranging from 7.4 to 11.3 μmol/L in NSCLC cells with wild-type *KRAS* and from 5.6 to 14.1 μmol/L in those with mutant *KRAS* (Fig. 1*A*), values that are within the clinically relevant concentration range for this drug (17). This inhibitory effect of sorafenib in cells with wild-type *KRAS* also seemed to be independent of whether the cells contained a mutant version of the *epidermal growth factor receptor* (*EGFR*) gene. We next investigated the effects of sorafenib on anchorage-independent colony formation in soft agar, a more clinically relevant model of NSCLC cell proliferation. Sorafenib inhibited anchorage-independent colony formation with IC_{50} values of 5.6 to 11.1 μmol/L in cells with wild-type *KRAS* and of 8.5 to 11.1 μmol/L in those with mutant *KRAS* (Fig. 1*B*). These data thus indicated that sorafenib inhibits the growth of NSCLC cells in a manner independent of *KRAS* mutational status.

To investigate the mechanism by which sorafenib inhibits NSCLC cell growth, we examined the cell cycle profile by flow cytometry. Sorafenib increased the proportion of cells in G_1 phase of the cell cycle and reduced that of cells in S or G_2-M phases in all tested cell lines regardless of *KRAS* mutational status (Fig. 2). Sorafenib did not increase the proportion of cells in sub-G_1 phase, a characteristic of apoptosis. These data thus indicated that sorafenib inhibits cell growth by inducing arrest of the cell cycle in G_1 phase.

Effects of sorafenib on the ERK signaling pathway in NSCLC cell lines. To examine the effects of sorafenib on the ERK signaling pathway in NSCLC cells, we performed immunoblot analysis with antibodies specific for phosphorylated (activated) ERK. Sorafenib markedly inhibited ERK phosphorylation in cells with wild-type *KRAS* regardless of the mutational status of *EGFR* (Fig. 3*A*). In contrast, sorafenib had no effect on the level of ERK phosphorylation in cells

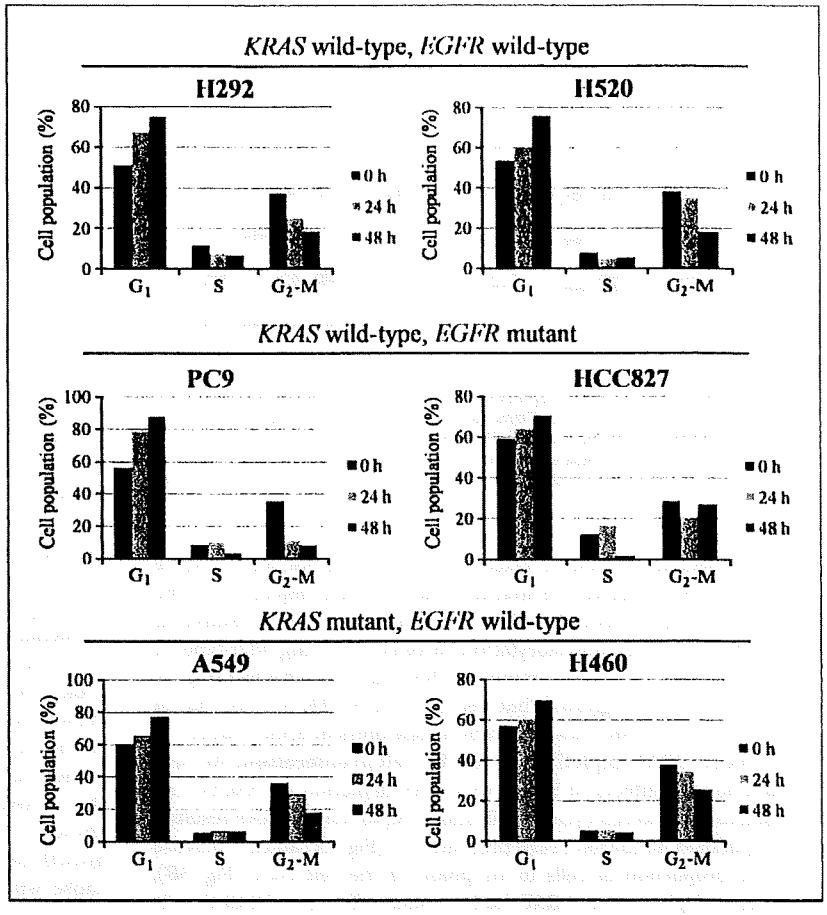

Figure 2. Effects of sorafenib on cell cycle distribution in NSCLC cells classified according to *KRAS* and *EGFR* status. Cells were incubated for 0, 24, or 48 h in complete culture medium containing 15 μmol/L sorafenib and were then fixed, stained with propidium iodide, and analyzed for cell cycle distribution by flow cytometry. All data are means of triplicates from representative experiments that were repeated on three separate occasions.

with mutant *KRAS*. To investigate further whether the effect of sorafenib on ERK phosphorylation is dependent on *KRAS* mutational status, we introduced an expression vector for FLAG epitope-tagged KRAS with the activating Val^{12} mutation (KRAS-V12) into the human NSCLC cell line H1299, which harbors wild-type endogenous *KRAS*. Whereas sorafenib inhibited ERK phosphorylation in nontransfected cells or cells transfected with the empty vector, it failed to do so in cells expressing KRAS-V12 (Fig. 3*B*). These results thus suggested that sorafenib blocks the ERK signaling pathway only in NSCLC cells harboring wild-type *KRAS*.

B-RAF but not C-RAF depletion inhibits ERK phosphorylation in NSCLC cells with wild-type or mutant KRAS. The mammalian RAF family includes A-RAF, B-RAF, and C-RAF, all of which function in the ERK pathway but also have different downstream phosphorylation targets and play distinct roles in signaling (18). Although suggested to be a B-RAF inhibitor, sorafenib inhibits the activity of C-RAF with a potency 4-fold that apparent for B-RAF (16). To investigate the downstream consequences of B-RAF and C-RAF signaling in NSCLC cells, we examined the effects of the depletion of these kinases with a siRNA-based approach. Immunoblot analysis revealed

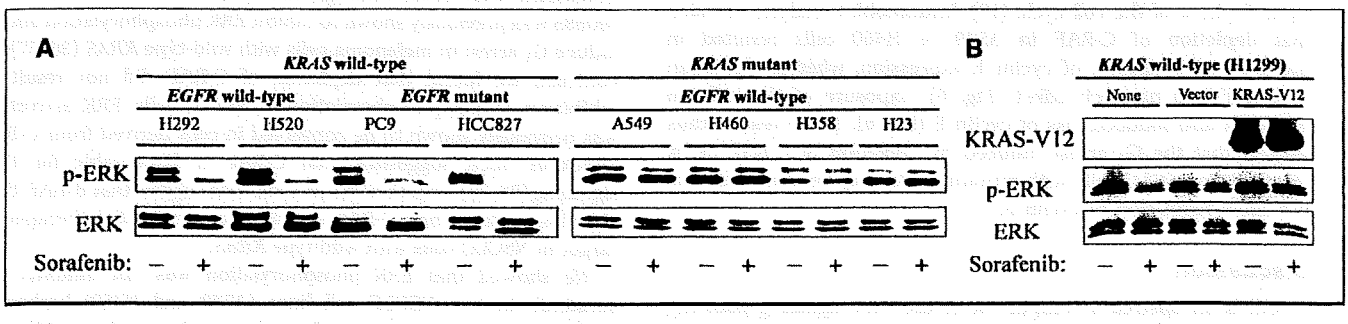

Figure 3. Effects of sorafenib on ERK phosphorylation in NSCLC cells classified according to *KRAS* and *EGFR* status. *A*, cells were incubated for 2 h in the presence or absence of sorafenib (15 μmol/L), after which cell lysates (25 μg of soluble protein) were subjected to immunoblot analysis with antibodies to phosphorylated (*p-ERK*) or total forms of ERK. *B*, H1299 cells were transiently transfected (or not) for 48 h with an expression vector for FLAG-tagged KRAS-V12 or with the corresponding empty vector and were then incubated for 2 h in the presence or absence of sorafenib (15 μmol/L). Cell lysates (25 μg of soluble protein) were then subjected to immunoblot analysis with antibodies to FLAG and to phosphorylated or total forms of ERK.